THE ASTROPHYSICAL JOURNAL, 277:648–674, 1984 February 15

THE SPECTRUM OF V348 SAGITTARII[1]

OVED DAHARI AND DONALD E. OSTERBROCK
Lick Observatory, Board of Studies in Astronomy and Astrophysics, University of California, Santa Cruz;
and Institute for Advanced Study, Princeton
Received 1983 June 13; accepted 1983 August 3

ABSTRACT

The unique irregular variable V348 Sgr was observed at various epochs. The faintest magnitude found was $V = 18.4$. It shows brightness changes of $\Delta V \geq 6.4$, which can occur within a few days. The spectrum is similar at maximum and minimum light, except for the forbidden lines, which remain at approximately constant brightness. In addition to the previously known C II and He I emission lines, a unique Ne I emission-line spectrum was observed. Using a curve of growth analysis, the abundance of C was found to be dominant in the chromosphere, with enhanced N and Ne abundances. The relation of this object to the R CrB stars and the Wolf-Rayet central stars of planetary nebulae is discussed. A model is suggested in which the original outer H-rich envelope had been expelled, and a final He-shell flash in the envelope of the remaining core formed a C-rich extended envelope. Dust clouds between the chromosphere and the H-rich planetary nebula cause the strong visible-light variations.

Subject headings: stars: abundances — stars: circumstellar shells — stars: evolution — stars: individual — stars: R Coronae Borealis — stars: variables

I. INTRODUCTION

V 348 Sgr is an irregular variable star, perhaps related to the R CrB type of variables. Its light curve was described by Hoffleit (1958). She found the photographic magnitude to vary from $V \approx 11$ to fainter than 16.5. The decline and rise times are approximately 7 days and 30 days, respectively. The average period or cycle time of V348 Sgr is ~ 200 days, so it stays most of the time near minimum or maximum light. However, the light curve is highly irregular. Heck, Houziaux, and Manfroid (1982), for example, found a decline from $V = 12$ to $V \geq 17$ in less than 4 days, followed by a recovery after less than a month. The image on the Palomar Sky Survey (PSS), which was taken at $V \sim 16$, shows a stellar-like source with a nebulosity clearly seen around it, especially in the red plate. The nebula is approximately 8″ in diameter.

Spectra were first obtained by Herbig (1958) on low-resolution plates. He reported rich C II and He I emission near maximum light, and a planetary nebula–like spectrum near minimum light, when the C II lines could no longer be detected. Houziaux (1968) obtained high-resolution spectrograms near maximum, and he also found a very rich emission-line spectrum of C II, as well as of other ions. He also resolved Hα, which was probably blended with C II λ6583 on Herbig's spectrograms.

Infrared photometry was reported by Feast and Glass (1973) and by Webster and Glass (1974). They found a very large infrared excess, with a blackbody temperature of approximately 800 K. The infrared brightness was found to remain approximately constant during all phases of the light curve.

Those spectra of Herbig (1958) and Houziaux (1968) were not calibrated for quantitative line-intensity measurements. None of their spectra were taken at minimum light, because of the faintness of the object. For the present paper we obtained spectrophotometric scans in various phases. In addition, Dr. Herbig kindly made available high-resolution CTIO spectrograms for our study.

II. OBSERVATIONS

Spectrophotometric scans were obtained with the Shane 3 m telescope at Lick Observatory, equipped with the image-dissector-scanner (IDS). The system is described by Miller, Robinson, and Schmidt (1980) and the data reduction is discussed, for example, by Osterbrock (1981). Gratings of 600 lines mm^{-1} and 1200 mm^{-1} were used, giving resolutions of approximately 10 Å and 5 Å, respectively, with spectral coverages of approximately 2550 Å and 1275 Å, respectively. The accuracy achieved with this system and the standard observing routine and data reduction is estimated at 10% in the line-flux ratios, 20% in the absolute flux (depends on weather conditions), and 1 Å in the wavelength scale.

V348 Sgr is at a declination of nearly −23°, and therefore it has a minimum zenith distance of nearly 57° at Lick Observatory. Hence it can be observed for only a few hours, near the meridian, and atmospheric dispersion is a very important consideration (see, for example, Filippenko 1982). The slit, 2.″7 × 4.″0 projected on the sky, was always aligned with the long axis approximately north–south through V348 Sgr, to minimize this effect. Even so, the slit size was too small to accept all the light, and various numbers of UV photons did not enter the slit (see also § IV*f*). Since the seeing, zenith distance, and atmospheric transmission at low altitude varied from one night to another, the uncertainty in the relative flux measurements (with respect to λ5536) increased toward shorter wavelengths to various extents, and could not be removed by any straightforward correction.

[1] *Lick Obs. Bull.*, No. 971.

TABLE 1

JOURNAL OF OBSERVATIONS

Date	V[a]	Instrument	Wavelength Range (Å)	Integration Time (min)	Resolution (Å)	$\frac{I_c(\lambda 5900)}{I_c(\lambda 7100)}$
1981 Jul 25/26	13.7	IDS	3500–5900	16	10	...
1981 Jul 25/26	13.7	IDS	4700–7100	16	10	1.08
1981 Aug 22/23	16.6	IDS	3500–5900	16	10	...
1981 Aug 22/23	16.6	IDS	4700–7100	16	10	1.05
1981 Oct 5/6	12.0	IDS	3500–5900	32	10	...
1981 Oct 5/6	12.0	IDS	4700–7200	16	10	1.21
1981 Oct 31/Nov 1	12.1	IDS	4700–7100	32	10	1.45
1981 Oct 31/Nov 1	12.1	IDS	3500–5900	16	10	...
1981 Nov 1/2	12.1	IDS	6000–8500	32	10	...
1981 Apr 10	15[b]	CTIO	5000–5900	62	1.3	...
1981 Apr 11	15[b]	CTIO	5850–6700	60	1.3	...
1981 May 21/22	16.4[c]	IDS	4900–7300	48	10	0.87
1981 May 21/22	16.4[c]	IDS	3500–5900	32	10	...
1981 Jun 14/15	18.4	IDS	3500–5900	32	10	...
1981 Jun 15/16	18.4	IDS	5800–7100	64	5	0.60
1981 Jun 15/16	18.4	IDS	4700–7100	32	10	0.58

[a] The method of calculating the visual magnitude is described in the text. I_c is the observed continuum intensity.
[b] Magnitude estimated by eye.
[c] Nonphotometric night.

However, since no other data of the blue part of the spectrum are available, we present the data as reduced. We estimate the fluxes reported for $\lambda \leq 4500$ Å to be only lower limits, with actual fluxes larger by a factor of 10 or more in some cases. Equivalent widths are still relatively accurate, as are relative fluxes of lines close to one another in wavelength.

High resolution spectra were obtained by G. H. Herbig with the 4 m telescope at the Cerro-Tololo Interamerican Observatory (CTIO). The telescope was equipped with a Carnegie image intensifier on the Cassegrain Ritchey-Chrétien spectrograph. Kodak IIIa-J emulsion was used, with a dispersion of 25 Å mm^{-1}, giving a resolution of approximately 1.4 Å.

The journal of observations is given in Table 1. The V magnitudes include the emission lines and were calculated by multiplying the scans by the V response curve of Johnson (1965). The zero points were determined by comparing the resulting integrated fluxes with those of the two standard stars which were observed at the beginning and end of each night. They were chosen from the Stone (1974, 1977) standards. We estimate the V values to be accurate to within ± 0.1 mag, with the largest uncertainty resulting from changes in transparency and seeing during the night. Applying the same method to the continuum only (after removing the emission lines), we found that the V continuum magnitudes are different from those of the total light by only ~ 0.02 mag and ~ 0.2 mag at $V = 12.1$ and $V = 16.6$, respectively. As a result, the V magnitudes of the continuum are larger by these differences.

The visual magnitude at the time the CTIO plates were taken is an eye estimate. It should be noted that the magnitude at minimum reported previously, $V \geq 17$, was only a lower limit. We obtained $V = 18.4$ at one epoch, but we cannot exclude a possibility of even a fainter phase.

Throughout this paper we use the visual magnitudes of Table 1 to identify the observing epoch under discussion.

III. SPECTRUM

Figures 1, 2, and 3 present the spectra taken with the IDS at $V = 12.1$, 16.6, and 18.4, respectively. The wavelengths are at the object's rest frame. In each figure, scans of different wavelength ranges are presented, with the flux scale adjusted to have the same average continuum level in overlapping regions. The ordinate scale in each figure was chosen such that the highest flux in the whole spectra has the full range. The high-dispersion scan is shown on the bottom of Figure 3, where it can be noted that Hα and the [N II], [S II] doublets are resolved.

a) Tables of Emission Lines

The line flux and equivalent width measurements are summarized in Tables 2–4, where we list the IDS and CTIO data separately. In the tables, W(Å) is the equivalent width, and the flux of the doublet C II λ5536 is given in units of 10^{-15} ergs s^{-1} cm^{-2} (above the Earth's atmosphere). In Table 3 (the CTIO spectrum), blanks are left if the line is not identified, and the uncertainty in W(Å) is on the order of 10%, mainly due to the uncertain continuum level. The emission lines were identified using redshifts and wavelengths of the strongest C II lines like λλ4267, 5890, 6580 as well as the lines of He I λλ5015, 6678, 7065. Weak lines in the region 5000–6900 Å were identified on the CTIO plates, where the wavelength scale is more accurate and the resolution is much better. When strong lines of the specific ion were present, other weak blended lines were assumed to be present. Blended lines in the IDS spectra were separated into components with a computer program, written originally by B. Hatfield, and subsequently modified by J. M. Shuder. The program produces a synthetic spectrum which best fits the data, using instrumental profiles from the comparison lamps taken with the same instrumental setup. The results were compared and averaged with those obtained with the standard Lick Observatory "deblend" computer program.

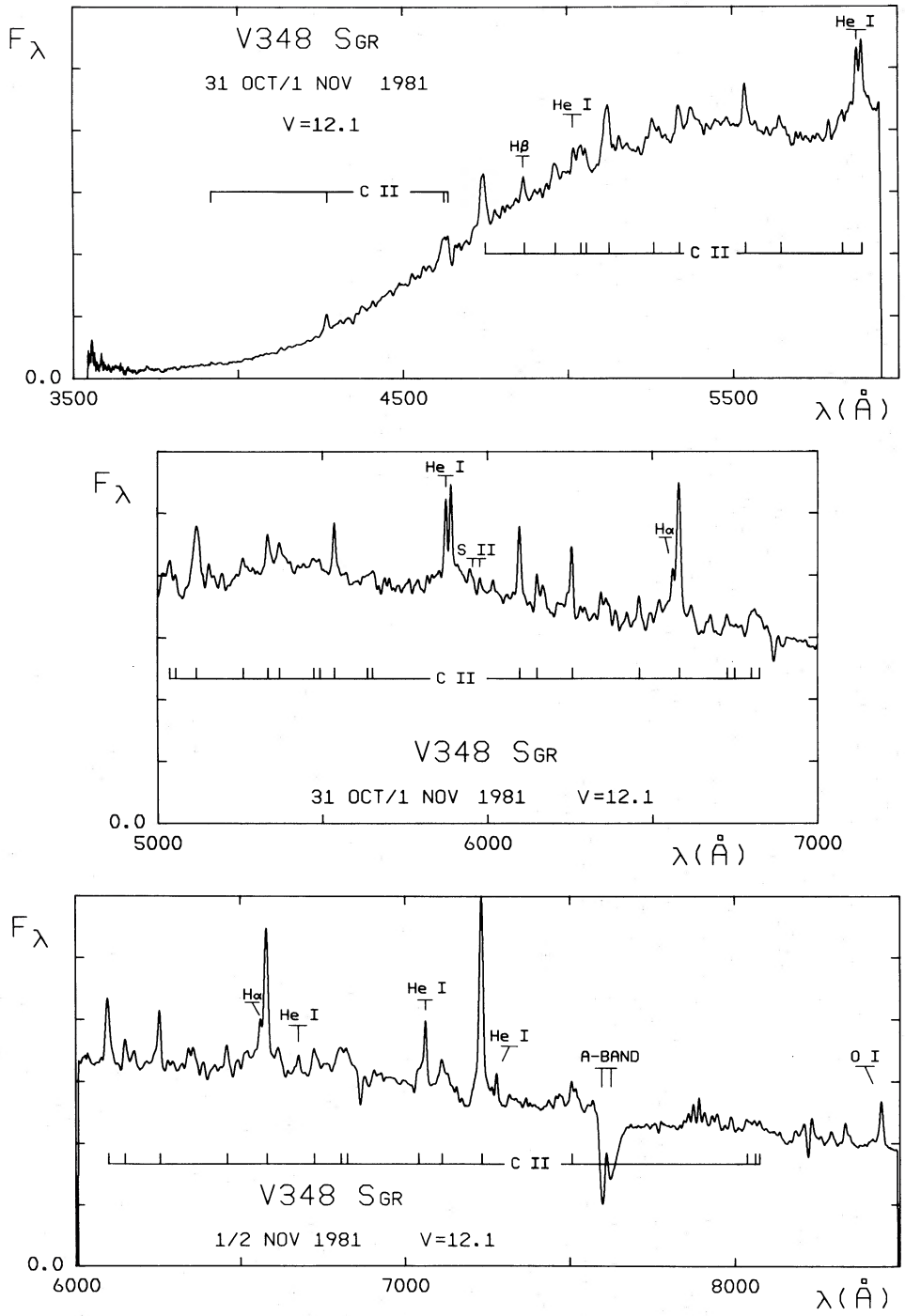

FIG. 1.—Bright phase. Continuum level at $\lambda 6500$ is $(45 \pm 10) \times 10^{-15}$ cm^{-2} Å^{-1}. The flux at the three figures was adjusted so the continuum level at overlapping regions is approximately the same. The atmospheric absorption A and B bands are still apparent after the division by the standard stars, due to the large zenith-distance differences. Note the weakness of [O II] $\lambda 3727$ doublet emission and the steep decline in flux toward the ultraviolet resulting from atmospheric dispersion. The identified C II lines are marked by tick marks from the horizontal line labeled C II.

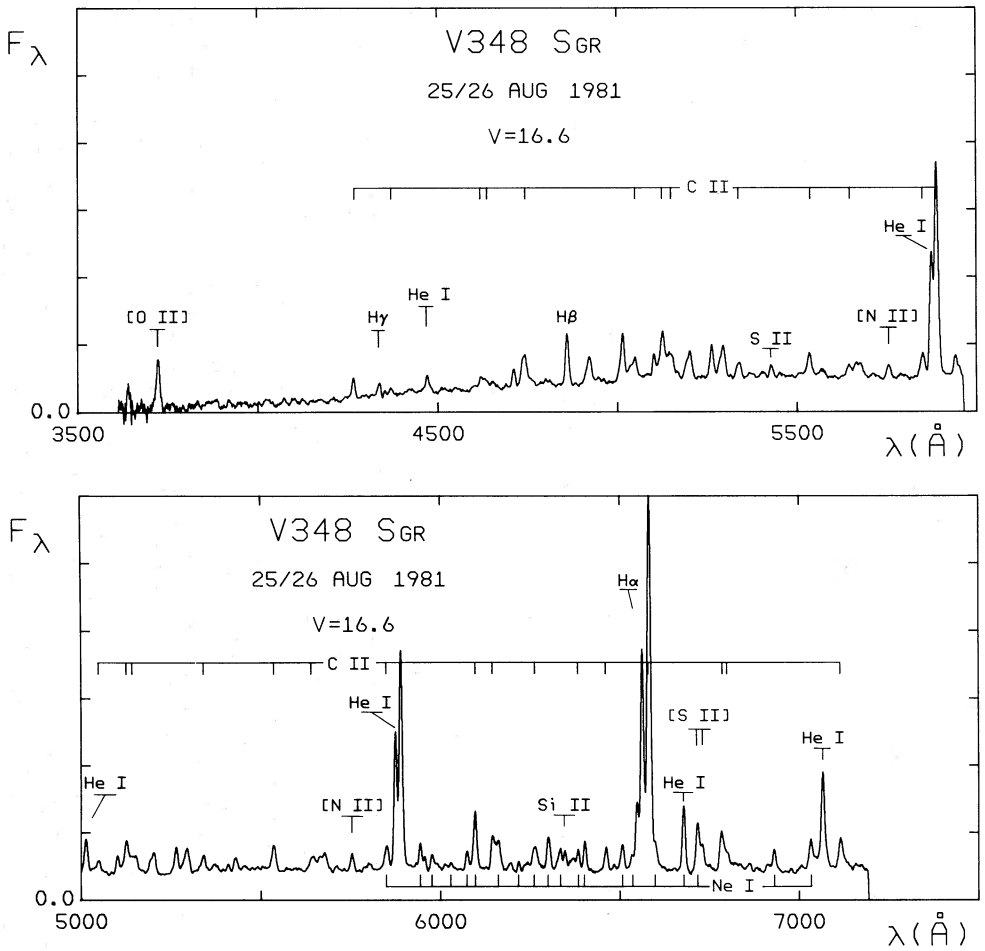

FIG. 2.—Intermediate phase. Continuum level at 6500 Å is $(0.7 \pm 0.2) \times 10^{-15}$ ergs s^{-1} cm^{-2} $Å^{-1}$. Flux is adjusted as in Fig. 1. The light curve at this observing epoch is known to be on a sharp decline. Ne I emission lines are very prominent.

Lines which were too weak or were separated by less then 3 Å could not be deblended in the 10 Å resolution scans. For deblended lines the uncertainty in the flux is approximately inversely proportional to the relative intensity in the blend. The intensities of [N II] λ6583 and [O I] λ6364 were assumed to be 2.95 and 0.32 times those of the measured [N II] λ6548 and [O I] λ6300, respectively, according to their transition probabilities.

The uncertainties in the line fluxes and equivalent widths given in Tables 2 and 4 are estimated by taking into account the problems discussed in § II, the accuracy achieved in the deblending process, and the continuum level determination, which was very difficult in some cases. The uncertainties in the relative line fluxes (and equivalent widths) are given by the letters *a*, *b*, and *c*, which stand for factors of 1.1, 1.4, and 2, respectively. When the uncertainties of the flux and equivalent width of a line are different, an additional appropriate letter is given for the uncertainty of the equivalent width (in parentheses). Note that the uncertainty of the flux of a whole blend is usually lower than those given for the individual lines in the blend. Upper limits are given for lines which are at or below the noise level. The line fluxes are given as ratios to the reference doublet C II λλ5535, 5538 (hereafter referred to as λ5536). This blend is chosen because it is not further blended, and it is present in the overlapping region of the "blue" and "red" scans. The flux listed for λ5536 is the average of its fluxes in those scans, and the uncertainty in its absolute flux (above Earth's atmosphere) is on the order of 20%.

The C II wavelengths and transitions were taken from Glad (1954). The multiplet numbers for C II and N II are taken from Moore (1970, 1975). Wavelengths and multiplet numbers of other elements are taken primarily from Wiese, Smith, and Glennon (1966, 1969).

b) *General Characteristics*

In general, the spectra of V348 Sgr consists of three components: the continuum, the permitted emission lines of C II and He I, and the forbidden emission lines. The continuum shape is uncertain below λ4500 due to the atmospheric dispersion problem described in § II. We therefore use the ratio of the continuum intensities I_c (in units of ergs s^{-1} cm^{-2} $Å^{-1}$) at λ5900 to λ7100 as a measure of the continuum slope. That wavelength range is only weakly affected by atmospheric dispersion (since the sensitivity of the television camera used for guiding on the slit peaks at 6000 Å),

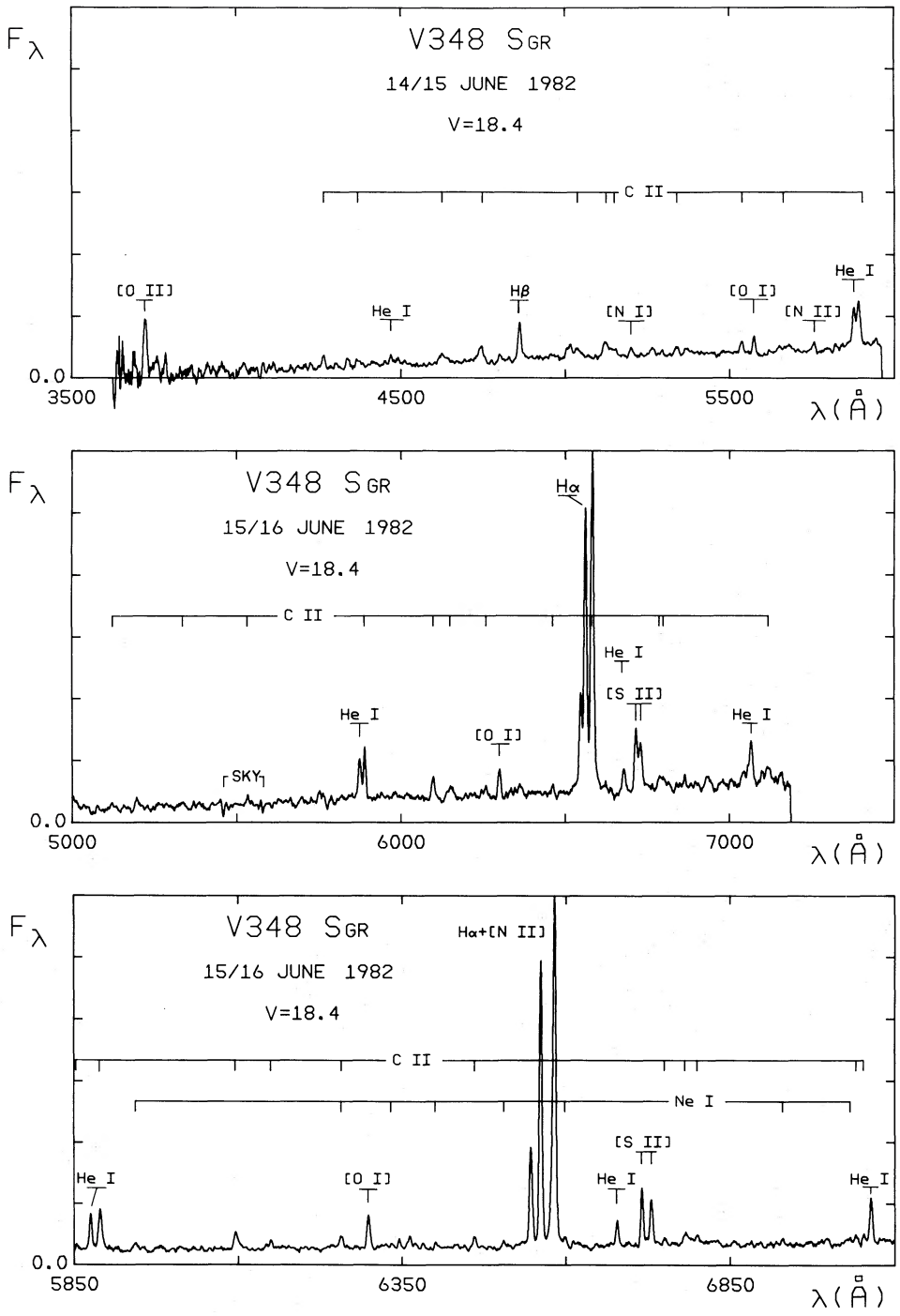

FIG. 3.—Faint phase. Continuum level at $\lambda 6500$ is $(0.4 \pm 0.3) \times 10^{-15}$ ergs s^{-1} cm^{-2} $Å^{-1}$. The flux of the top two figures was adjusted as in Fig. 1. The bottom figure shows the high dispersion scan (resolution ~ 5 Å). C II and He I are still detected in emission, and Ne I emission lines are suspected as well.

TABLE 2

IDS EMISSION LINES*

Laboratory Wavelength (Å)	ID	Multiplet	25 July '81 F (5536) = 27.7 R	25 July '81 EW(Å)	22 Aug '81 F (5536) = 6.31 R	22 Aug '81 EW(Å)	5 Oct '81 F (5536) = 103.5 R	5 Oct '81 EW(Å)	31 Oct '81 F (5536) = 127 R	31 Oct '81 EW(Å)	22 May '82 F (5536) = 3.0 R	22 May '82 EW(Å)	14 June '82 F (5536) = 1.1 R	14 June '82 EW(Å)
3726.0 3728.8	[O II]		0.84c	5.0(a)	1.8c	115	<0.1	<3	0.07c	4.7(b)	3.3c	CD	6.39c	360(b)
3888.8	He I	2	0.48c	1.9(a)	<0.1	<5	<0.1	<2	<0.01	<0.4	<0.3	-	<0.3	<3
3919.0 3920.7	C II	4	0.96c	3.6(a)	<0.1	<4	0.22c	3.5(b)	0.013c	0.54	<0.3	<5	<0.5	<5
4076.4	C II	36	<0.1	<0.4	0.12b	4.2	<0.1	<2	<0.01	<0.4	CD	-	CD	-
4267.0 4267.3	C II	6	1.8c	4.7(a)	0.57b	12.3	0.71c	4.0(a)	0.31c	3.8a	0.4b	5.7	1.07c	11(b)
4340.5	Hγ	1	0.1	0.25	0.32c	5.9	<0.1	<0.6	BLD	-	0.2	2.3	0.74c	6.9(b)
4368.1 4369.0 4370.7 4372.4 4374.3 4375.0 4376.6	C II	45 + 46	0.27b	0.66(a)	0.16b	2.8	0.2	1.0	CD	-	0.32b	3.1	0.31c 0.27c	2.6 2.3
4409.2 4410.0	C II	40	<0.2	<0.7	<0.1	1.8	CD	-	CD	-	<0.1	<1.0	<0.2	<1.2
4411.2 4411.5 4413.3	C II	39												
4471.5	He I	14	<0.2	<0.7	0.53b	7.75	<0.1	<0.3	BLD	-	<0.1	<1.0	0.46c	3.3(b)
4618.4 4619.2	C II	49 + 50	0.81b	1.8	0.40c	5.3	0.07c	0.26	0.33b	1.7	0.1c	0.7	<0.2	<1
4625.6 4627.4 4630.0	C II	49 + 50	0.88b	2.0	0.27c	3.6	0.47b	1.74	0.19c	1.0	0.3b BLD	2.1 -	0.87c	6.0
4367.6 4638.9	C II	12.01	BLD	-	0.22c	2.9	0.23c	0.85	0.12c	0.64	0.46a	3.13	0.55c	3.8
4713.2	He I	12	BLD	-	0.40b	4.75	BLD	-	BLD	-	<0.1	<0.9	<0.1	<0.8
4727.4 4734.6	C II	48	1.4b	3.2	BLD	-	0.57b	1.8	0.67b	2.2	0.6b	3.7	<0.2	<1
4735.5 4738.0	C II	1			0.55b	6.5							0.4c	2.0
4744.8 4747.3	C II	1	1.7b	3.9	1.0b	11	1.34b	4.5	1.18b	3.9	0.91b	5.5	1.0b	5.0

TABLE 2—*Continued*

Laboratory Wavelength (Å)	ID	Multiplet	25 July '81 F (5536) = 27.7		22 Aug '81 F (5536) = 6.31		5 Oct '81 F (5536) = 103.5		31 Oct '81 F (5536) = 127		22 May '82 F (5536) = 3.0		14 June '82 F (5536) = 1.1	
			R	EW(Å)	R	EW(Å)	R	EW(Å)	R	EW(Å)	R	EW(Å)	R	EW(Å)
4861.3	Hβ	1	0.65b	1.4	1.5b	19.4	0.6b	1.5	0.40c	1.15	1.42a	6.2	3.7b	18.4
4862.6 4867.1	C II	10.01	0.25c	0.6	BLD	-	0.25c	0.6	0.18b	0.52	BLD	-	0.80b	4.0
~4912.0	?		<0.1	<0.25	0.25c	3.2	<0.1	<0.3	<0.05	<0.15	<0.15b	0.76	<0.05	<0.2
4921.9	He I	48	0.23b	0.61	0.7b	9.1	<0.1	<0.3						
4948.9	[O III]	-	CD	-	0.08c	0.9	CD	-	0.05	0.15	0.2c	0.71	0.14c	0.36
4953.8 4958.7 4959.9 4964.7	C II	25	0.35b 0.24b	0.71 0.48	<0.05	<0.5	0.29c 0.38b	0.6 0.7	0.07c 0.31b 0.22b	0.18 0.82 0.58	0.4b	1.7	<0.1	<0.4
5006.7	[O III]		<0.1	<0.2	0.26c	2.3	0.08c[+]	0.16	BLD	-	0.6c	2.3	0.69b	1.8
5015.7	He I	4	0.90b	2.0	1.4b	12.2	0.47b	0.97	0.51b	1.3	0.93	3.6	1.24b	3.2
5032.1 5035.9 5040.7	C II	17	0.42c	0.94	0.25c	2.2	0.50b	1.04	0.37b	0.93	0.51b	2.0	0.7c	1.8
5041.8	C II	35												
5046.1	He I	47	0.6b	1.33	0.25c	2.2	0.57b	1.18	0.36b	0.9	0.42c	1.6	0.7c	1.8
5044.3 5045.0 5047.1 5049.2	C II	35	0.24c	0.56	0.46b	4.0	0.25b	0.50	0.26c	0.65	0.30b	1.15	0.34c	0.9
~5103.0	?	-	0.25c	0.64	0.60a	5.7	<0.1	<0.2			0.1c	0.35	<0.1	<0.3
5107.9 5113.7 5114.3 5116.7 5119.4	C II	50.03 + 51	BLD 0.21c	- 0.42	BLD 0.14c	- 1.43	BLD 0.24b	- 0.41	0.08c	0.19	0.55b	1.9	0.18c	0.4
5120.1 5121.8	C II	12	1.07b	2.2	0.27c	2.2	0.93b	1.6	1.00b	2.40	0.44c	1.54	0.85b	2.2
5122.5	C II	16.06	BLD	-										
5125.2 5126.9	C II	12	0.45b	0.92	0.5c	4.1	0.34c	0.58	0.90b	2.14	0.5c	1.75	0.8c	2.1

TABLE 2—*Continued*

Laboratory Wavelength (Å)	ID	Multiplet	25 July '81 F (5536) = 27.7		22 Aug '81 F (5536) = 6.31		5 Oct '81 F (5536) = 103.5		31 Oct '81 F (5536) = 127		22 May '82 F (5536) = 3.0		14 June '82 F (5536) = 1.1	
			R	EW(Å)	R	EW(Å)	R	EW(Å)	R	EW(Å)	R	EW(Å)	R	EW(Å)
5132.9	C II	16	0.19c	0.39	0.8c	0.6	0.38b	0.65	BLD	-	0.55b	1.9	0.45c	1.2
5133.3														
5137.3			0.21c	0.43	0.14c	1.1	BLD	-			0.46b	1.6	0.56c	1.5
5139.2														
5143.5			BLD	-	0.6c	4.9	0.24b	0.41	<0.05	<0.15				
5145.2					0.42c	3.4	BLD	-						
5151.1														
~5154.1	?	-	0.52a	1.20	0.14c	1.25	0.28b	0.6	0.24b	0.57	0.24b	0.84	0.56c	1.5
5202.3	Si II[+]	23	CD	-	1.2a	12.0	<0.1	<0.2	<0.05	<0.1	<0.1	<0.35	0.95b	4.0
5249.5	C II	30	0.11c	0.27	1.3b	12.1	<0.2	<0.4	0.1c	0.2	BLD	-	<0.1	<0.4
5253.6														
5256.1			0.47b	1.27			0.74b	1.4	0.3b	0.7	0.4b	1.3	0.6b	1.8
5257.2														
5259.1														
5259.7														
~5263.5	?		0.11c	0.27					0.1c[+]	0.2	0.2b	0.66		
5286.5	C II	56	0.35b	0.80	0.43c	4.0	<0.2	<0.4	<0.05	<0.1	<0.1	<0.3	<0.1	<0.3
5290.1					1.0b	9.3	<0.1	<0.2			CD	-		
~5294.8	?	-	BLD	-									0.2b	0.6
5332.9	C II	11	0.40b	0.75	BLD	-	0.16b	0.28	1.0a	2.28	0.37b	1.2	0.2c	0.6
5334.8														
5339.8	C II	17.07	0.43c	1.0	0.64a	6.3	0.63b	1.08	0.1b	0.23	0.49b	1.6	0.4c	1.2
5342.4	C II	17.06												
5368.6	C III	16.05	0.6b	1.2	0.2b	2.0	0.37c[†]	0.75	0.3b	0.7	1.08a	3.5	0.3c	0.9
5380.0	C I[+]	11	0.5b	1.0	<0.1	<1.0	0.30c[†]	0.55	0.2b	0.45	0.4b	1.3	0.15c	0.45
5428.6	S II	6	0.35c	0.85	0.38b	4.0	0.25b	0.44	CD	-	<0.1	<0.3	<0.05	<0.15
5432.8														
5478.6	C II	34	0.22b	0.52	<0.2	<2.0	0.41b	0.7	0.15b	0.35	0.12c	0.4	<0.1	<0.3
5483.3							0.08c	0.16			0.18c	0.6		
5485.9			<0.1	<0.2			0.24c	0.45			0.31b	1.0		
5488.9														
5490.2														
5535.3	C II	10	1.0a	2.18	1.0a	9.2	1.0a	1.82	1.0a	2.25	1.0b	3.5	1.0b	3.8
5537.6														
5547.6	?		<0.1	<0.2	<0.1	<0.9	0.07b	0.13	0.1c	0.2	0.15c	0.5	<0.05	<0.2

TABLE 2—*Continued*

Laboratory Wavelength (Å)	ID	Multiplet	25 July '81 F (5536) = 27.7 Å		22 Aug '81 F (5536) = 6.31 Å		5 Oct '81 F (5536) = 103.5 Å		31 Oct '81 F (5536) = 127 Å		22 May '82 F (5536) = 3.0 Å		14 June '82 F (5536) = 1.1 Å	
			R	EW(Å)	F	EW(Å)	R	EW(Å)	R	EW(Å)	R	EW(Å)	R	EW(Å)
~5634.0	?		0.16b	0.33	BNL	-	0.05c	0.1	<0.05	<0.1	<0.1	<0.3		
5640.5	C II	15	0.08c	0.20	0.17c	1.7	0.15b	0.27	0.15b	0.35	0.40b	1.3	<0.2	<0.8
5648.1			0.29b	0.69	0.45b	4.4	0.22b	0.4	0.15b	0.35				
5662.5			0.13c	0.31	0.40b	4.0	0.23b	0.4	0.05c	0.1	0.37b	1.2		
5666.6	N II	3	<0.1	<0.2	0.27b	2.7	0.1c	0.2	<0.05	<0.1			<0.1	<0.4
5679.6			<0.1	<0.2	0.44b	4.4	<0.1	<0.2	CD	-	0.5c	1.65	0.6b	2.1
5686.2			<0.1	<0.2	0.17c	1.7	CD	-	CD	-			0.15c	0.6
5710.8			<0.1		0.15b	1.5					BNL	-		
5747.3	N II	9	0.13b	0.3	0.09c	0.85	CD	-	CD	-	CD	-	0.2c	0.7
5754.6	[N II]	-	0.11b	0.25	0.34b	3.37	CD	-	CD	-	CD	-	0.7b	2.5
5767.4	N II	9	0.07c	0.17	0.05c	0.5	CD	-	<0.05	<0.1	CD	-	<0.1	<0.4
5791.8	C II	58	0.05c	0.11	<0.2	<2.0	CD	-	0.2b	0.5	CD	-		
5818.3	C II	22	BLD	-	<0.1	<1.0	CD	-	CD	-	CD	-	<0.1	<0.4
5823.1														
5827.8					0.12c	1.12								
5836.3					0.11	1.02							0.1c	0.42
5843.6														
5856.0														
5852.5	Ne I	6	0.2c	0.4	0.29b	2.7	<0.1	<0.2	CD	-				
5875.6	He I	11	2.05a	4.2	4.35b	39	1.75a	3.2	1.22a	2.6	0.87a	2.3	3.12a	12.9
5881.9	Ne I	1	BLD	-	0.16c	1.43	BLD	-	BLD	-	BLD	-	BLD	-
5889.3	C II	5	3.12a	6.3	5.28b	47.2	2.0a	3.6	1.40a	3.0	1.04a	2.75	4.03a	16.7
5889.8					2.6b	23.2								
5891.6														
5907.2	C II	44.01	BLD	-	0.15c	1.4	<0.1	<0.2	BLD	-	CD	-	<0.1	<0.4
5914.6			<0.1	<0.2	<0.1	<1.0								
5919.4														
5944.8	Ne I	1	0.18c	0.38	0.65b	5.8	0.1b	0.2	0.4c	0.86	CD	-	0.46b	1.9
5957.6	Si II	4	0.16c	0.3	0.21b	1.9	0.13b	0.25						
5975.6	Ne I	1	<0.05	<0.1	0.42b	3.8	0.1	0.2	0.14b	0.3	<0.1	<0.3	0.4b	1.7
5978.9	Si II	4												
6030.0	Ne I	3	0.13b	0.3	0.13b	1.1	0.18b	0.3	<0.05	<0.1	0.2b†	0.6	<0.1	<0.4
6018.0	?		<0.1	<0.2	<0.1	<0.8	CD	-	0.2b	0.42	<0.1	<0.3		
6074.3	Ne I	3	CD	-	0.58a	5.6	<0.1	<0.2	CD	-	<0.1	<0.3	<0.1	<0.4

TABLE 2—*Continued*

Laboratory Wavelength (Å)	ID	Multiplet	25 July '81 F (5536) = 27.7		22 Aug '81 F (5536) = 6.31		5 Oct '81 F (5536) = 103.5		31 Oct '81 F (5536) = 127		22 May '82 F (5536) = 3.0		14 June '82 F (5536) = 1.1	
			R	EW(Å)	R	EW(Å)	R	EW(Å)	R	EW(Å)	R	EW(Å)	R	EW(Å)
6096.16	Ne I	3	0.16c	0.4	0.82b	7.9			BLD	-	0.18c	0.4	0.86c	3.1
6095.3	C II	24	1.3b	3.1	1.05b	10.2	2.47	3.5	1.04b	2.8	1.64a	3.6	2.0b	7.1
6098.5			0.3c	0.7	0.17c	1.6	0.1	1.3	0.47c	1.3				
6102.6														
6143.1	Ne I	1	<0.1	<0.25	1.1b	10.4	<0.1	<0.2	<0.05	<0.1	<0.1	<0.25	0.88c	3.3
6151.43	C II	16.04	0.41b	1.0	0.62c	5.9	0.7b	1.14	0.48b	1.3	0.73b	1.55	2.1b	7.9
6163.6	Ne I	5	0.71b	1.71	0.98b	9.3	0.6b†	0.1	BLD	-	0.4b	0.88	0.3c	1.13
6175.0	N II	36	<0.1	<0.2	<0.1	<1.0	0.1c†	0.16	0.48b	1.3				
6217.3	Ne I	1	0.05c	0.1	0.14b	1.37	CD	-	CD	-	0.36b†	0.8	<0.1	<0.4
6246.6	C II	38.03	0.17c	0.42	<0.1	<1.0	0.5c	0.9	CD	-	<0.1	<0.2	0.4c	1.3
6250.7									0.25c	0.69				
6256.5														
6253.8	C II	43.03	1.07c	2.6	BLD	-	1.2b	2.1			0.2c	0.4	1.0b	3.3
6257.2	C II	10.03			0.82b	7.5			0.81a	2.2	1.64a	3.5		
6259.6														
6266.5	Ne I	5	BLD	-	0.36c	3.3	<0.1	<0.17	BLD	-	<0.1	<0.2	<0.1	<0.3
6300.3	[O I]	-	0.15b	0.4	1.16a	10.7	<0.1	<0.2	0.06b	0.13	1.2a	2.54	3.1b	10.7
6304.8	Ne I	3									BLD	-		
6305.5	S II	19									BLD	-		
6334.4	Ne I	1	<0.05	<0.1	0.77a	7.4	CD	-	CD	-	<0.1	<0.2	0.3c	0.9
6347.1	Si II	2	0.37b	0.9	0.53a	4.7	0.6b	1.2	0.36b	0.99	0.80b	1.7	0.3c	0.9
6363.8	[O I]	-	0.52c	1.3	0.47b	4.5	0.4b	0.8	0.52b†	1.43	0.4a	0.85	0.8b	2.5
6371.4	Si II	2	BLD	-							0.82b	1.75	0.5c	1.5
6383.0	Ne I	3	0.11c	0.26	0.56a	5.4	0.4b	0.8	CD	-	BLD	-	<0.1	<0.3
6385.7	C II	55												
6402.2	Ne I	1	CD	-	0.87a	8.4	<0.1	<0.2	<0.05	<0.1	<0.1	<0.2	<0.1	<0.3
6454.8	C II	17.05	0.43b	1.1	BLD	-	BLD	-	BLD	-	BLD	-	<0.1	<0.3
6461.9	C II	17.04			0.75.a	7.3	1.12a	1.9	0.43b	1.2	1.15a	2.5	0.66a	2.0
6482.1	N II	8	CD	-	0.13b	1.2	CD	-	CD	-	<0.1	<0.2	<0.1	<0.3

TABLE 2—*Continued*

Laboratory Wavelength (Å)	ID	Multiplet	25 July '81 F (5536) = 27.7 Å		22 Aug '81 F (5536) = 6.31 Å		5 Oct '81 F (5536) = 103.5 Å		31 Oct '81 F (5536) = 127 Å		22 May '82 F (5536) = 3.0 Å		14 June '82 F (5536) = 1.1 Å	
			R	EW(Å)	R	EW(Å)	R	EW(Å)	R	EW(Å)	R	EW(Å)	R	EW(Å)
6506.5	Ne I	3	CD	–	0.87a	8.4	BLD	–	BLD	–	CD	–	<0.1	<0.3
~6518.5	?				<0.1	<1.0	0.63a	1.02	0.22b	0.45				
6532.9	Ne I	5			0.47c	4.2	BLD	–	BLD	–				
6548.1	[N II]	–	0.75b	1.8	2.16b	19.2	0.37b	0.6	0.31c	0.87	3.5a	6.5	11.3a	28.2
6562.8	Hα	1	2.6b	6.2	8.06a	71.5	1.71a	2.75	0.76b	2.1	8.5a	15.9	32.a	80.8
6578.0, 6582.9	C II	2	3.4a	8.1	6.22b, 3.13b	55.2, 27.8	4.25b	6.84	2.2b	6.2	0.67c	1.25	13.0b	32.4
6583.4	[N II]	–	2.25b	5.4	6.5b	57.5	1.16b	1.87	0.93c	2.6	10.5a	19.7	33.8a	84.3
6598.9	Ne I	6	CD	–	1.0c	8.8	0.4c†	0.64	BLD	–	BLD	–	BLD	–
~6619.0	?	–	CD	–	<0.1	<1.0	0.2b	0.3	0.30b	0.84	0.1c†	0.2	<0.1	<0.3
6678.1	He I	46	0.78a	1.9	2.24a	22.2	0.8b	1.4	0.37b	1.0	0.37c	0.76	3.0a	8.5
6678.3	Ne I	6												
6716.4	[S II]	–	0.1c	0.25	1.7b	16.2	0.04c†	0.07	BLD	–	1.8a	3.5	7.35a	19.0
6717.0	Ne I	6												
6730.8	[S II]	–			0.95b	8.1	0.9b†	1.62	BLD	–	1.96a	3.9	5.7a	14.7
6724.6, 6727.2, 6731.1, 6733.6, 6734.0	C II	21	0.56b	1.4	BLD	–	CD	–	0.25b, 0.25b	0.66, 0.66	BLD	–	<0.03	<1.0
6738.6, 6742.4, 6750.5, 6755.2	C II	21	BLD	–	<0.2	<2.0			CD	–	0.2c†, 0.5c†	0.4, 1.0		
6779.9, 6780.6, 6783.9	C II	14	CD	–	0.7b	6.5	<0.1	<0.2	CD	–	<0.1	<0.2	BLD	–
6787.2, 6791.5	C II	14	0.20c	0.5	0.83b, 0.35c	7.7, 3.25	0.31c	0.5			0.24c	0.45	1.0b	2.3
6798.1, 6800.7	C II	14	0.51b	1.3	0.59b	5.5	1.33b	2.2	0.36b	1.0	0.76, BLD	1.44, –	0.66b	1.54
6812.3	C II	14	0.24c	0.6	0.19c	1.8	0.08c	0.14	0.40b	1.1	0.66b	1.25		
~6820.0	?		0.53c	1.3	<0.1	<1.0	1.38b	2.3	0.5c	1.4	0.35c	0.66	<0.1	<0.25
6929.5	Ne I	6	0.25b	0.63	0.7a	6.75	0.46a	0.7	<0.05	<0.1	<0.1	<0.2	<0.1	<0.25
7032.4	Ne I	1	BLD	–	1.14a	10.3	<0.1	<0.2	<0.05	<0.1	<0.1	<0.2	<0.1	<0.25

TABLE 2—*Continued*

Laboratory Wavelength (Å)	ID	Multiplet	25 July '81 F (5536) = 27.7 R	25 July '81 EW(Å)	22 Aug '81 F (5536) = 6.31 R	22 Aug '81 EW(Å)	5 Oct '81 F (5536) = 103.5 R	5 Oct '81 EW(Å)	31 Oct '81 F (5536) = 127 R	31 Oct '81 EW(Å)	22 May '82 F (5536) = 3.0 R	22 May '82 EW(Å)	14 June '82 F (5536) = 1.1 R	14 June '82 EW(Å)
~6990.0	?		<0.1	<0.2	<0.1	<1.0	<0.1	<0.2	<0.05	<0.1	0.4b	0.74	<0.1	<0.25
7046.3	C II	26	0.44c	1.1	0.27c	2.4	0.39b	0.71	0.26c	0.85	0.3c	0.5	2.1b	4.6
7053.1	C II	26	0.13c	0.3	0.42c	3.8	0.57b	1.04	0.27c	0.9	0.5c	0.9	0.24c	0.5
7063.7	C II	26	1.7b	4.1	0.82c	7.4	2.2a	3.9	1.1b	3.6	1.62b	2.9	5.7b	12.1
7065.2	He I	10			3.03b	27								
7112.5	C II	20												
7113.0	C II	20	0.46b	1.13	0.56b	5.0	1.0b	1.8	0.42c	1.4	0.47c	0.86	0.55c	1.13
7115.6	C II	20			0.30b	2.7								
7119.9	C II	20	0.15c	0.37	0.06c	0.5	0.4c	0.7	0.40b	1.3	0.75c	1.37	1.5b	3.08
7125.7	C II	20	0.33b	0.81	0.25b	2.2								
7132.4	C II	20	0.27b	0.66	0.11c	1.0	0.4c	0.7	0.13c	0.4	0.65c	1.18		
7134.1	C II	20									0.50c	0.9	<0.2	<0.4
7144.2	C II	20	0.33b	0.81	<0.1	<1.0	<0.1	<0.2	0.06c	0.2	0.74	1.34		
~7215	?								<0.1	<0.4	0.7c	1.4		
7321.3	C II	3							2.2b	7.2	4.0b	7.9		
7236.4	C II	3							2.62b	8.5	2.9b	5.7		
7237.2	C II	3												
7281.3	He I								0.32b	1.1	0.9a	1.7		
7319.0	[O II]	2F							0.07b	0.24				
7330.0	[O II]	2F							CD	-				
7461.75	C II	17.1							0.16b	0.6				
~7472.8	?								0.23b	0.86				
~7480	?								0.18b	0.67				
7508.9	C II	16.08							0.39b	1.45				
7519.7	C II	16.08							0.19c	0.7				
7530.6	C II	16.08							0.05c	0.2				
~7862.5	?								0.16b	0.80				
~7877.6	?								0.28b	1.4				
~7894.9	?								0.33c	1.7				
~7910.8	?								0.21b	1.05				
~7934.3	?								0.14b	0.73				
~7949.1	O I^{+}	35							0.21b	1.05				
~7973.0	?								0.04b	0.22				
~7991.5	O I^{+}	19							0.20a	1.05				

TABLE 2—*Continued*

Laboratory Wavelength (Å)	ID	Multiplet	25 July '81 F (5536) = 27.7 R	25 July '81 EW(Å)	22 Aug '81 F (5526) = 6.31 R	22 Aug '81 EW(Å)	5 Oct '81 F (5536) = 103.5 R	5 Oct '81 EW(Å)	31 Oct '81 F (5536) = 127 R	31 Oct '81 EW(Å)	22 May '82 F (5536) = 3.0 R	22 May '82 EW(Å)	14 June '82 F (5536) = 1.1 R	14 June '82 EW(Å)
8028.9	C II	27.02							BLD	-				
8037.7									0.25b	1.1				
8039.4														
8048.3									0.18c	0.8				
8062.1									0.24b	1.1				
8062.8														
8076.6									0.29	1.3				
8294.5	?								0.21b	1.0				
8337.4	?								0.24b	1.1				
8343.0	?								0.11c	0.4				
8446.5	O I								0.86a	4.3				

* Multiplet numbers are taken from Moore (1970, 1975). W(Å) is the equivalent width. Flux values are given as ratios to the C II doublet λ5535. The flux of that doublet is given in units of 10^{-15} ergs s^{-1} cm^{-2} (above Earth's atmosphere) and is accurate to within a factor of 1.2 (see text).
R, Ratio of the emission-line flux over F(5536).
BLD, Line is to weak to be deblended.
CD, Line is weak, and its flux could not be determined due to uncertain continuum determination.
† Identification is uncertain due to wavelength discrepancy.
a, *b*, *c*, Uncertainty by a factor of 1.1, 1.4, and 2, respectively.
~ : Approximate wavelength of nonidentified line in the object's rest frame.

TABLE 3

CTIO SPECTRUM

λ(meas.)	W(Å)	ID(mult.)	λ(lab.)	$V_\odot$	Notes	λ(meas.)	W(Å)	ID(mult.)	λ(lab.)	$V_\odot$	Notes
5018.12	3.00	HeI(4)	5015.67	146	1	5261.76	1.05	CII(30)	5259.71	117	9
5028.43	0.48	NII(19)	5025.67	165	6	5267.32	0.65	MgII(17)	5264.14	181	5, 3
5034.35	1.10	CII(17)	5032.07	136	5	5272.62	0.46	FeIII(112)	5269.15	197	6, 3
5038.06	0.99	CII(17)	5035.91	128	5	5287.37	0.75	AlII(102)	5285.83	85	3, 6, 5
5043.48	1.41	CII(17) SiII(5)	5040.74 5041.03		8	5292.68	0.10	CII(56)	5290.09	147	3, 4
5046.54	0.50	CII(35) NII(4)	5044.35 5045.1		8	5296.58	0.68				1
5050.08	1.04	HeI(47) CII(35)	5046.1 5047.11+49.24		8	5303.07	0.60	FeIII(113)	5302.5		3, 6
5053.79	0.53					5309.05	0.20				
5058.57	0.58	SiII(5)	5055.98	154		5323.16	0.11				1
5076.14	0.46	NII(10) FeIII(5)	5073.59 5073.78	151	8, 1	5335.45	1.09	CII(11)	5332.89	144	9
5086.77	0.14					5337.05	1.85	CII(11)	5334.79	127	9
5089.27	0.24	FeIII(5)	5086.69	152	3	5344.81	2.53	CII(17.06)	5342.40	135	3
5094.05	0.05				6	5351.11	0.14				6, 4
5101.98	0.30	CaII(16)	5099.30	158	4, 3	5370.73	1.23	CII(16.05)	5368.58	120	3
5105.08	0.63	CaII(16)	5103.04	120	1	5373.42	0.63	AlII(42)	5371.84	88	9, 3
5109.83	0.41	CII(51)	5107.91	113	4, 3	5377.33	0.82				
5116.42	2.28	CII(50.03)	5113.69	-	4, 2	5382.72	0.56				5
5122.18	1.95	CII(50.03)	5119.45	160	9	5384.66	0.23				1, 9
5124.18	2.21	CII(50.03)	5121.82	-	9, 8	5388.97	0.32				6
5129.56	3.56	CII(12)	5125.2 +26.9	-	2, 8	5392.62	0.34				
5135.75	1.65	CII(16)	5133.28+32.94	-	2, 6	5399.70	0.45				6, 2
5140.5	2.46	CII(16)	5137.26+39.17	-	2, 6	5403.3	0.32	NeI(3)	5400.56	152	6
5146.79	2.66	CII(16)	5143.49+45.16		1	5412.19	0.27				6
5153.69	1.42	CII(16)	5151.09	152		5428.90	0.30				
5158.45	1.72	FeIII(5)	5156.0	142	3	5432.35	0.42	SII(6)	5428.64	205	5
5163.47	0.39				6	5435.26	0.30	SII(6)	5432.77	137	5
5171.16	0.40	NII(70)	5168.24	169	2	5445.27	0.61	CaII(2)	5443.42	102	3, 1
5178.18	0.44	NII(66)	5175.89	133	2, 3	5449.2*	0.20				6, 2
5181.00	0.34	NII(66)	5179.52	85	3	5456.47	0.36	SII(6) NII(29)	5453.81 5452.08+54.2		8
5187.91	0.40	SiII(7.14)	5185.53	137		5469.65	0.28	SiII(7.03)	5466.87+66.43	-	
5195.86	0.71	SiII(23) FeIII(5)	5192.86 5193.89+94.43		1, 8, 3	5475.56	0.21	SII(6)	5473.59	108	5
5202.98	0.21				5, 4	5481.02	0.64	CII(34) NII(29)	5478.59 5480.06+78.10		5, 1
5206.65	0.78	SiII(23)	5202.41	244	1, 3	5485.57	0.11	CII(34)	5483.35	121	4
5252.49	0.29	CII(30)	5249.51	170		5488.34	0.21	CII(34)	5485.90	133	
5255.99	0.35	CII(30)	5253.57	138	5	5498.23	0.27	SiII(32) NII(29)	5496.45 5495.67	-	8, 3
5259.86	0.70	CII(30)	5257.24	149	9	5511.97	0.13	SII(6)	5509.67	125	4

TABLE 3—*Continued*

λ(meas.)	W(Å)	ID(mult.)	λ(lab.)	V_Θ	Notes	λ(meas.)	W(Å)	ID(mult.)	λ(lab.)	V_Θ	Notes
5537.94	2.47	CII(10) NII(63)	5535.35 5535.36	140	9, 8 3	5982.07	0.81	SiII(4)	5978.93	157	1
5539.95	2.00	CII(10)	5537.61	126	9	5991.45	0.26				2, 6
5547.61	0.74				6	5995.74	0.49				
5585.85	0.16					6002.48	0.41				8
5588.0*	0.14				6	6023.19	0.35				5
5597.7*	0.18				6	6064.33	0.25	A&II(99)	6061.11		3
5595.96	0.17	A&II(16)	5593.23	146		6071.73	0.10	A&II(92)	6068.46	162	8
5608.30	0.17	SII(11)	5606.11	117	6, 4	6077.44	0.23	NeI(3) A&II(92)	6074.34 6073.23		1, 3
5636.95	0.26					6081.12	0.36	SiII(29)	6080.06	52	3
5643.15	1.52	CII(15) SII(11,14)	5640.55 5640.32+39.96		8	6088.0*	0.13				
5650.56	1.22	CII(15)	5648.07	132	1	6093.47	0.37				2, 6
5662.23	0.21	SII(11)	5659.95	121		6098.23	1.71	CII(24)	6095.29	147	9
5665.10	1.00	CII(15) SII(11)	5662.47 5664.73		8, 1 3	6101.35	3.16	CII(24)	6098.51	140	9, 5
5669.29	0.38	NII(13)	5666.63	141		6105.34	1.01	CII(24)	6102.56	137	5
5678.45	0.34	NII(3)	5676.02	128	4	6108.75	0.34				6
5682.24	0.90	NII 3)	5679.56	141	1, 6	6116.58	0.21				
5688.87	0.46	NII(3)	5686.21	140		6130.39	0.15				6
5713.60	0.70	NII(3)	5710.77	149	1, 6	6147.49	0.25	NeI(1)	6143.06	216	1
5749.95	0.37	NII(9)	5747.30	138		6154.14	1.90	CII(16.04)	6151.43	132	5
5757.22	0.53	[NII]	5754.57	138	3	6167.53	0.10	NeI(1)	6163.59	192	4
5769.76	0.47	NII(9)	5767.44	120		6170.28	0.59	NII(36)	6167.76	122	
5878.92	5.02	HeI	5878.62	169	1, 5	6172.79	0.1	NII(36)	6170.17	127	5
5889.85*	0.10	NaI	5889.95		5	6176.04	0.30	NII(36)	6173.31	132	5
5893.74	6.23	CII(5)	5889.77+91.59		8	6178.96	0.15				5
5897.46*	0.08	NaI	5895.92		5	6184.16	0.27	A&II(66)	6183.42+82.4		6, 3
5900.33	0.70				6, 7	6209.0*	0.08				
5910.37	0.46	CII(44)	5907.21	161	6	6215.16	0.78				6, 8
5916.92	0.26	CII(44)	5914.64	115	5	6220.29	0.25	Ne I(1)	6217.28	145	
5922.84	0.16	CII(44)	5919.45	172	4	6223.20	0.54				
5932.29	0.18	NII(28)	5927.81	227	4	6229.11	0.37	A&II(10)	6226.18	141	
5933.97	0.17	NII(28)	5931.78	110	6, 4	6234.71	0.64	A&II(10)	6231.78	140	5, 1
5944.4	0.28	NII(28)	5941.65+40.24			6238.65	0.26				5
5948.09	0.90	NeI(1)	5944.83	164	1	6241.79	0.25	SiII(7.13)	6239.63	104	4
5960.03	0.43	SiII(4)	5957.56	124	5	6245.96	0.71	NII(57) A&II(10)	6242.41 6243.36		8
5973.33	0.25	A&II(100)	5971.94	70	3	6253.77	0.72	CII(38.08)	6250.74	145	1
5978.21	0.15	NeI(1)	5975.53	134	6	6260.03	2.2	CII(10.03)	6257.18	137	9, 5

TABLE 3—*Continued*

λ(meas.)	W(Å)	ID(mult.)	λ(lab.)	$V_\odot$	Notes	λ(meas.)	W(Å)	ID(mult.)	λ(lab.)	$V_\odot$	Notes
6262.32	2.65	CII(10.03)	6259.59	131	9, 5	6401.15	0.15	SII(19) CaII(58)	6397.7 6399.41		6, 8 3
6269.97	0.34	NeI(5)	6266.49	166	4, 6	6406.02	0.32	NeI(1)	6402.25	177	1
6273.63	0.12				4	6427.98	0.36				
6275.10*	0.15				6	6458.29	0.28				1, 6
6282.61	0.28				1, 5	6461.78*	0.18				
6287.32	0.51	NII(32)	6284.32	143	3	6464.87	1.87	CII(17.04)	6461.95	135	1, 5
6301.16	0.25	SKY[OI]	6300.32	-	1	6485.03*	0.15	NII(8)	6482.05	138	
6304.16	0.20	[OI]	6300.32	183	5	6487.64	0.09				1
6307.85	0.23	SII(19)	6305.51	111	1	6498.43	0.14				1
6330.45	0.25	NII(46)	6328.39	98	3, 1	6506.73	0.09	NII(45)	6304.61	98	3, 6
6338.73	0.11	NeI(1) AlII(22)	6334.43 6335.74		3, 8	6510.41	0.07	NeI(3)	6506.53	179	5
6343.54	0.27	NII(46)	6340.57	140	3, 5	6523.01*	0.05				5
6350.04	1.45	SiII(2)	6347.10	139	1	6525.32	0.57	CaII(59)	6522.38	135	3, 1
6359.91	0.61	NII(46)	6356.54+57.57		3	6544.90*	0.12				
6363.72	0.53	SKY[OI]	6363.81			6550.39	0.90	[NII]	6548.06	107	3, 6
6366.44	0.40	[OI]	6363.81	124	4	6559.06	0.29				2
6374.20	0.53	SiII(2)	6371.36	139	1	6566.07	4.42	Hα	6562.82	149	1
6383.25*	0.15					6581.85	5.81	CII(2)	6578.05	173	9, 8
6387.74	0.66	CII(55) SII(19)	6385.72 6384.89		3, 8	6586.46	8.69	CII(2) [NII]	6582.88 6583.39		9, 1
6391.18	0.15				4	6624.70	0.31	CII(17.03)	6622.05	120	3, 4
6395.23	0.44				1	6681.33	1.73	HeI	6678.15	143	6

The measured wavelength and radial velocity ($V_\odot$) are corrected to the Earth's motion. W(Å) and multiplet numbers are the same as in Table 2. Uncertainties in W(Å) are all in the level of 10%, mainly due to continuum level determinations. Blanks were left when the line is not identified.

Notes. (1) Red asymmetry. (2) Blue asymmetry. (3) Uncertain identification. (4) Weak, close to noise level. (5) Sharp line. (6) Broad line. (7) Shallow, broad. (8) Possible blend of a few lines. (9) W(Å) uncertain—blend.

* Absorption line.

and the image-tube response is good. The continuum-ratio values for the various epochs are listed in Table 1. The continuum slope is correlated with the brightness, in the sense that the brighter the star is, the "hotter," or less reddened, it becomes.

The C II and He I emission lines have approximately the same relative fluxes at all epochs for which we have spectral scans. The C II + He I emission-line equivalent widths are generally approximately constant. An exception is the phase $V = 16.6$, when the star was fading rapidly and the C II and He I emission lines had significantly larger equivalent widths.

The width of the emission-line profiles could be measured with confidence only on the CTIO high-dispersion spectrograms. The intrinsic full widths at half-maximum (FWHM) of the C II emission lines are 65 ± 15 km s^{-1}, and the FWHM of the Ne I emission lines (as well as Hα) are 100 ± 20 km s^{-1}.

c) Ne I

The Ne I emission spectrum is clearly seen on several spectral scans, as well as on the CTIO plates. The Ne I lines were especially strong at $V = 16.6$, where their equivalent widths were quite large (see Table 1 and Fig. 2). In general, the relative intensities in the Ne I spectrum are fairly similar to those in the neon comparison lamp. However, some lines are different, for example λ6402, which is weaker in the object's spectrum relative to other lines. The Ne I lines are relatively broad in the CTIO spectra, and are very weak or absent near maximum light.

d) C II

The C II spectra are almost complete. Basically all the strong lines in the region 5040–6730 Å, measured by Glad

TABLE 4

ABSORPTION LINES[a]

1981 July 25 $V = 13.5$				1981 October 5 $V = 12.0$				1981 October 31 $V = 12.1$			
λ_{meas}[b]	F[c]	W(Å)	unc.[d]	λ_{meas}	F	W(Å)	unc.	$\lambda_{meas.}$	F	W(Å)	unc.
3999.0	9.1	1.1[b]	c								
4095.5	7.3	0.8[a]	b								
4317.8	7.5	0.65	b	4318.7	14.5	0.7	b	4317.4	5.25	0.42 (b)	c
4348.6	15.6	1.32	b	4593.8	25.1	1.1	b	4347.5	13.9	1.05 (b)	c
4593.8	7.8	0.63	a	4347.6	30.8	0.97	a	4589.3	12.4	0.5	b
4647.0	9.0	0.63	b	4648.0	41.5	1.25	b	4648.3	25.9	0.95	c
5076.5	14.2	1.0	b[e]					5074.3	51.5	1.1	e
5310.0	3.5	0.25	b	5310.3	4.0	0.07	c				
5413.6	6.8	0.5	b	5417.1	8.6	0.16	b	5414.4	12.4	0.23	b
				5591.5	10.4	0.19	b				
								5681.2	27.8	0.53	b
6044.3	2.3	0.2	c					6049.2	9.6	0.2	c
6481.3	4.4	0.35	b	6481.1	27.0	0.45	b	6480.8	21.2	0.46	c
				6642.5	30.4	0.54	b	6640.0			
6987.7	5.1	0.4	a	6992.0	19.3	0.35	b				
				7015.1	23.2	0.43	c				

[a] Only lines that are clearly stronger than the noise level are included. For suggested identifications see text. Blank is left when a line is not prominent below the continuum, or the continuum level is highly uncertain, or both (cf. Fig. 1).

[b] Corrected for redshift by neighboring identified emission lines.

[c] Flux given in units of 10^{-15} ergs s^{-1} cm^{-2} above the Earth's atmosphere.

[d] Uncertainties as in Table 2.

[e] Broad, continuum level uncertain.

(1954, 1956) in the laboratory, appear in the CTIO spectrum. In the IDS spectra in the wavelength region 4100–8500 Å, basically all the C II lines that are strong in the laboratory (Glad 1954) are present at at least one epoch. However, the line-flux ratios within the C II multiplets are sometimes quite different from those observed in the laboratory. It is interesting to compare the laboratory and stellar spectra in detail.

There are two main differences between the lines that arise from the C II singly and doubly excited configurations ($1s^2 2s^2 nl$ and $1s^2 2s2pnl$, respectively). (i) Lines from singly excited transitions are slightly asymmetric toward the red at $V = 15$, as is the He I λ5875 line. (ii) At $V = 16.6$, the lines from singly excited levels are enhanced ($\lambda\lambda$5890, 6580 for example) compared with the doubly excited lines.

e) *The Forbidden Lines*

The forbidden lines seem to have approximately the same absolute flux at all phases. As a result, they are not prominent at maximum, since their equivalent widths are at or below the noise level.

The forbidden-line spectrum resembles that of a planetary nebula with extremely low ionization, even lower than IC 418 (Kaler 1976). [O III] $\lambda\lambda$4959, 5007 is very weak or absent. Since the He I emission lines do *not* stay at the same flux level at various epochs, most of their photons probably originate not from the same region as the forbidden lines, but rather from the C II emitting region. It is apparent that the He I emission from the forbidden-line region is very weak. The line at λ5202 (Table 2) is probably a blend of [N I] λ5198 with Si II λ5202 (23), but certain identification could not be achieved.

f) *Absorption Lines*

A few absorption lines are detected in our data only at $V \leq 13.5$. In most cases the absorption lines are weak, and the continuum level determination is difficult. In Table 4 we list those lines which could be distinguished from the continuum with some confidence, and blanks are left when they were below the noise level (see also Fig. 1).

We used the atlas of stellar spectra by Morgan, Keenan, and Kellman (1943) for identification, assuming the underlying continuum is stellar. We propose identifications for the following lines: $\lambda\lambda$4318, 4350 are O II absorption lines (multiplets 4 and 16, respectively), and λ4648 is O II + C III (both multiplet 1). These lines are prominent in the spectra of B0–B1 supergiants. Using that identification, we could also verify the presence of weak O II $\lambda\lambda$6721, 6640, 4595, 4415, Si III λ4552, and Si IV λ4089. The weakness of the He I and H I absorption lines can be explained by abundance deficiencies and/or superimposed emission. However, the absence of the multiple O II λ4073 (10) in the spectra shed some doubt on the spectral type determination. The B0–B1 spectral type we obtained is consistent with the dereddened UBV colors given by Houziaux (1968). (He identified λ6481 in absorption as N II.)

The CTIO spectrum shows very few suspected absorption lines. None of the absorption lines in Table 4 is seen in the CTIO spectrum (note the limited wavelength range). There is no evidence for "inverse P Cygni" profiles, reported by Houziaux, for any of the emission lines on our CTIO plates. Those disagreements could be understood from the different phases of the light curve, especially since the exact phase (rising, falling, etc.) was not known for our observation epochs

TABLE 5

RADIAL VELOCITIES[a]

	C II			He I			H I			Ne I			[N II] + [S II]		
EPOCH	$\langle V \rangle$	σ	n	$\langle V \rangle$	σ	n	$\langle V \rangle$	σ	n	$\langle V \rangle$	σ	n	$\langle V \rangle$	σ	n
1981 Jul 25	133	17	6	147	33	6	...	...	...	153	40	3	...	...	...
1981 Aug 21	129	27	6	171	37	6	179	17	2	169	27	9	187	12	3
1981 Oct 5	123	29	6	171	65	6	...	...	...	...	...	...	...	...	...
1981 Oct 31	141	47	8	142	52	6	...	...	...	...	...	...	...	...	...
1982 Apr 10	144	18	25	156	11	4	149	...	1	172	24	10	...	...	...
1982 May 21	162	47	4	108	59	5	142	8	2	...	...	...	154	48	3
1982 Jun 15	147	14	6	161	22	6	94	...	1	177	30	4	152	22	4

[a] For each ion, $\langle V \rangle$ is the averaged velocity in km s^{-1} with respect to the Sun, σ is the standard deviation, and n is the number of the (not blended) lines used in the statistics.

except for $V = 16.6$ (Heck, Houziaux, and Manfroid 1982), when the light curve was in a rapid decline.

In the CTIO spectrum, the Na I $\lambda\lambda$5890, 5896 (measured wavelengths) absorption lines are clearly seen on both wings of C II λ5890 (which is redshifted to λ5893), and are probably interstellar in nature. That indicates a nonnegligible amount of interstellar reddening (see § IV*e*).

g) *Radial Velocities*

Table 5 gives the radial velocity measurements in the rest frame of the Sun. Only unblended lines were used, and for each ion the average radial velocity $\langle V \rangle$, the standard deviation σ, and number of lines used n, are listed. The standard deviations found are in accord with the expected errors of the wavelength calibration for the IDS system (Osterbrock 1981).

IV. DISCUSSION

a) *Optical Depth Effects*

The C II multiplets λ4740 (1) and λ6580 (2) have the same upper term, and their measured line ratio at $V = 16.6$ is $F(\lambda 6580)/F(\lambda 4740) = 6.0 \pm 0.5$ (this ratio is even smaller at other epochs). However, C II λ4740 is a two-electron transition $2s2p^2\ ^2S \leftarrow 2s^23p\ ^2P^o$, forbidden under the one-electron jump selection rule. Nussbaumer and Storey (1981) calculated the transition probabilities A for these lines, with configuration interaction taken into account. They found $A(\lambda 6580) = 3.6 \times 10^7\ \text{s}^{-1}$, $A(\lambda 4740) = 7.9 \times 10^4\ \text{s}^{-1}$. The calculated line ratio for an optically thin gas is therefore $F(\lambda 6580)/F(\lambda 4740) \approx 3.3 \times 10^2$. As they stated, λ4740 is expected to be extremely weak, if not unmeasurable, in any optically thin astrophysical source.

$A(\lambda 4740)$ is the least well determined of any in their calculations, and they estimated its "minimum measure of uncertainty" as about 30%, but presumably it is not in error by a factor of over 50. The great strength of λ4740 in V348 Sgr therefore indicates strong optical depth effects, in which λ4740 photons are generated by repeated scattering and fluorescence of other photons, presumably mostly in the $2s2p^2\ ^2D \leftarrow 2s^23p\ ^2P^o$ λ1760 (UV 10) and $2s2p^2\ ^2S \leftarrow 2s^23p\ ^2P^o$ λ2838 (UV 13) multiplets. One or both transitions must be optically thick in the envelope of V348 Sgr. Unfortunately, neither of them is in the region observable from the ground, and the estimated reddening makes V348 Sgr quite faint for *IUE* ultraviolet observations (see § IV*e* below). The observed λ6580 may or may not be optically thick; its transition probability is comparable with those of λ1760 and λ2838, but its lower excitation potential is greater. (See also § IV*c*.)

The He I line ratio $F(\lambda 7065)/F(\lambda 3889) = 3.5 \pm 2$ at $V = 13.5$ when λ3889 is prominent. The equivalent-width ratio of these lines is 2.2 ± 0.2. Both are much larger than the value of 0.15 given by Osterbrock (1974, hereafter *AGN*) for this line ratio in the case B recombination spectrum of He I. The difference cannot be explained by any reasonable reddening or atmospheric refraction effect. Feldman and MacAlpine (1978) investigated the optical depth effects on the He I spectrum in the context of a *dense* gaseous nebula. On the basis of their results, we conclude that the optical depth of He I λ10830 is of the order of 50–100. (It would be interesting to observe this line in the infrared.) We conclude that He I λ3889 is also optically thick and relatively weak for that reason. This line is known to be very prominent in the spectra of R CrB variables, especially near minimum light. This could indicate a significant difference between the physical conditions of V348 Sgr and these variables (see also § V).

The permitted line O I λ8446 arises partly from resonance fluorescence of Lyβ. Netzer and Penston (1976) discuss the intensity ratio λ8446/Hα, and find that it increases with the optical depth in Hα as well as the abundance of O. They find typical values of the line ratio $\lambda 8446/\text{H}\alpha = 10^{-2}$ with solar abundances and $\tau(\text{H}\alpha) \approx 10^{2.5}$. O I λ8446 is very prominent in V348 Sgr at $V = 12.1$, the only time we observed it in the infrared. The line flux ratio λ8446/Hα is found to be 1.2 ± 0.2. The absence of other permitted O I lines [for example, λ7002 (21)] in the spectra of V348 Sgr rules out the stellar-continuum fluorescence mechanism suggested by Grandi (1975). It also suggests that the large optical depths in Hα and Lyβ are the prime cause of the strong λ8446 emission in V348 Sgr, although its relative strength to Hα is probably enhanced by the relatively low abundance of H.

b) *The Nature of the* C II *Emitting Region*

The presence of the rich C II emission, especially the *quartet* multiplets [for example, λ7120 (20), λ6800 (14), λ5650 (15)], can be explained in the following three ways:

1. *Recombination.* The ground configuration of C^{++} is $1s^22s^2\ ^1S$. Neither normal radiative recombination nor di-electronic recombination with this ion can produce the quartet terms of C^+ (see Seaton and Storey 1976). However, the first

excited term of C^{++} is $1s^2 2s2p\,^3P^o$ at 6.5 eV, which can recombine into the quartet terms of C^+. That triplet level is significantly populated when the temperature and density are above 2×10^4 K and 10^3 cm^{-3}, respectively. Also, C must be mostly in the form C^{++}, and ultraviolet radiation with $h\nu \geq 24$ eV is needed to balance the recombinations. Supportive of this possible mechanism is the fact that, in V348 Sgr, emission lines from terms of higher L are relatively strong. [Examples are $2s2p3s\,^4P^o \leftarrow 2s2p3p\,^4D$ λ6780 (14), and $2s2p3p\,^4D \leftarrow 2s2p3p\,^4F^o$ λ7120 (20).] The absence of C III emission lines could be explained by their high excitation potentials ($h\nu \geq 29$ eV), but a strong C III] λ1909 emission line is expected in this case.

2. *Fluorescence.* A second possible explanation for the presence of C II quartets could be relatively high temperature and density, with C in the form C^+. Then the metastable term $2s2p^2\,^4P$ with excitation potential 5.3 eV would be collisionly populated. In this case the higher quartet levels could be populated by ultraviolet radiative fluorescence, and would emit the optical line radiation. Here the ultraviolet photon energies needed are of order 18 eV. This interpretation does not explain the strength of $2s^24f\,^2F^o \leftarrow 2s^26g\,^2G$ λ6462 (17.04), which cannot be induced by radiative fluorescence from the ground level of C^+.

3. *LTE.* The third possible explanation could be more or less the same physical conditions as in case 2 above, but with the density high enough so that the higher terms of C^+ are collisionly populated. This would occur in a chromosphere that is close to LTE. Basically no high-energy radiation is needed in this case, but the density must be 10^{15} cm^{-3} or higher. That possibility seems most likely, and hence we discuss it further below.

c) *Curve of Growth Analysis*

In order to examine the physical conditions in the C II emission-line region, we try to match a curve of growth (COG) plot to the C II (and Ne I) emission lines, assuming the emission does not depend on the background continuum. We outline the relatively idealized theory in the Appendix. The abscissa of the COG is $X = \log(gf\lambda) - (\chi)(\log e)/kT$, where χ is the excitation energy of the transition's lower level above the reference level, which was chosen arbitrarily for convenience. The ordinate is $\log\{F(\text{line})/[B_\lambda(T)\cdot\lambda]\}$, where F(line) is the emitted flux in the line, and $B_\lambda(T)$ is the blackbody emission at the wavelength λ. Since the distance to V348 Sgr is unknown, the absolute emission intensity at the stellar surface is not known, so we take the flux values above the Earth's atmosphere as given in Table 2. Hence the ordinate of the COG has an unknown constant shift which is proportional to the solid angle of the object.

The energy levels for C II are taken from Wiese, Smith, and Glennon (1966). The C II lines and the gf-values (Mühlethaler 1977) used for the COG analysis are listed in Table 6, where the multiplet numbers are the same as in Table 2. We did not use lines with $\lambda < 4500$ because of their uncertain flux. Mühlethaler gives gf-values for each multiplet, but not for each line. (His values are listed in col. [4].) We calculated each line's fraction of the multiplet's gf-value using the relative strength tables of Allen (1963, p. 56). Only prominent lines of the multiplet are used. In some cases, the wavelength separation between lines within a multiplet is less than 1 Å. When one line is dominant, the line in Table 6 is actually a blend, and the gf-value listed is the sum of the gf-values in the blend. (Here the error which originates from the nonlinearity of the COG is estimated as much smaller than the uncertainty in the flux measurement.) In cases where two close unresolved lines have comparable gf-values (i.e., $\lambda\lambda$4637, 4639), we estimated their relative strength using the data from the CTIO spectra, or assumed the relative strength as in Allen's tables.

The data points in the COG are sensitive to the effective temperature T in the emitting region and to the reddening correction. To correct for reddening, we use the expression (see *AGN*, p. 171):

$$F_0(\lambda) = F(\lambda)\exp[Cf_r(\lambda)]\,,$$

where $F_0(\lambda)$ is the corrected line flux, C is the reddening coefficient [$C \approx 1.39(E_{B-V})$], and $f_r(\lambda)$ corresponds to the coefficient f in equation (7.5) in *AGN*, so that $f_r = f + 0.43$. [Since the ordinate of the COG is logarithmic and arbitrary,

TABLE 6

C II LINES USED IN THE CURVE OF GROWTH ANALYSIS[a]

Line	Mult.	gf (line)	gf (mult.)	Line	Mult.	gf (line)	gf (mult.)
4637	12.01	0.030	0.0895	5648	15.00	0.37	...
4639	12.01	0.054	...	5662	15.00	0.56	...
4737	1.00	0.0014	0.0041	5844	22.00	0.021	0.234
4745	1.00	0.0028	...	5856	22.00	0.093	...
5133	16.00	1.36	4.72	5889	5.00	0.67	1.20
5137	16.00	0.13	...	5892	5.00	0.40	...
5139	16.00	0.21	...	6098	24.00	1.75	2.92
5144	16.00	2.31	...	6103	24.00	0.195	...
5151	16.00	0.708	...	6151	16.04	1.75	1.75
5333	11.00	0.010	0.0313	6251	38.03	0.689	1.14
5335	11.00	0.021	...	6257	10.03	0.038	0.114
5342	17.07	0.798	0.798	6260	10.03	0.069	...
5535	10.00	0.036	0.0553	6462	17.04	2.56	2.56
5538	10.00	0.018	...	6578	2.00	0.92	1.39
5640	15.00	0.187	1.12	6583	2.00	0.46	...

[a] The multiplet numbers are the same as in Table 2. For the gf values listed, see text, § IVc.

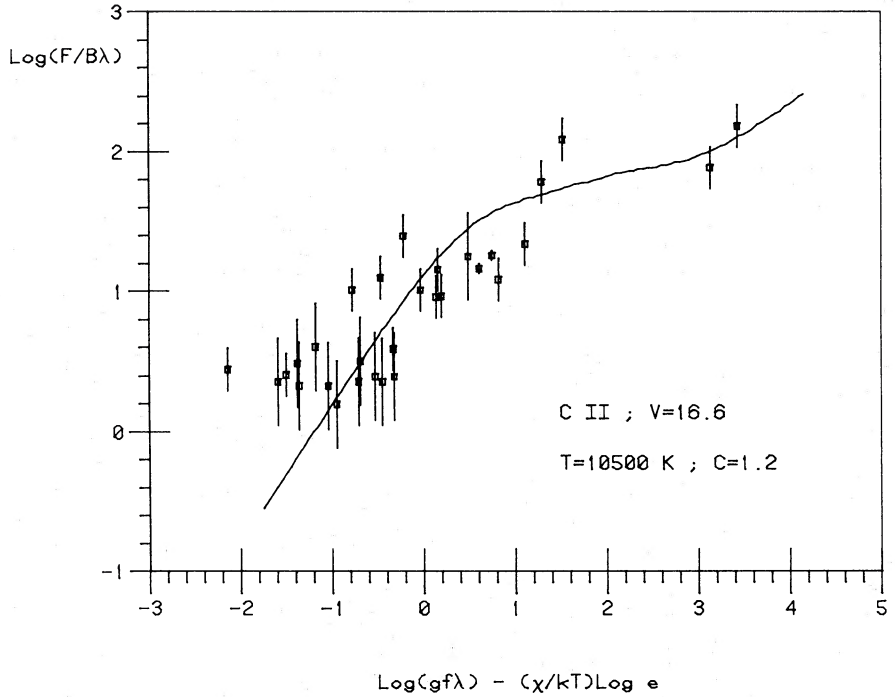

FIG. 4.—Curve of growth for the C II emission lines at $V = 16.6$. χ is the lower energy level of each transition, assuming $\chi = 0$ for the reference energy level $1s^2 2s 2p^2\ ^2P$. The flux uncertainties are taken from Table 2, $T = 1.05 \times 10^4$ K, and $C = 1.2$ (see text). The solid line is taken from Powell (1969) with $a = 0.005$, shifted by 6.4 vertically and 5.2 horizontally.

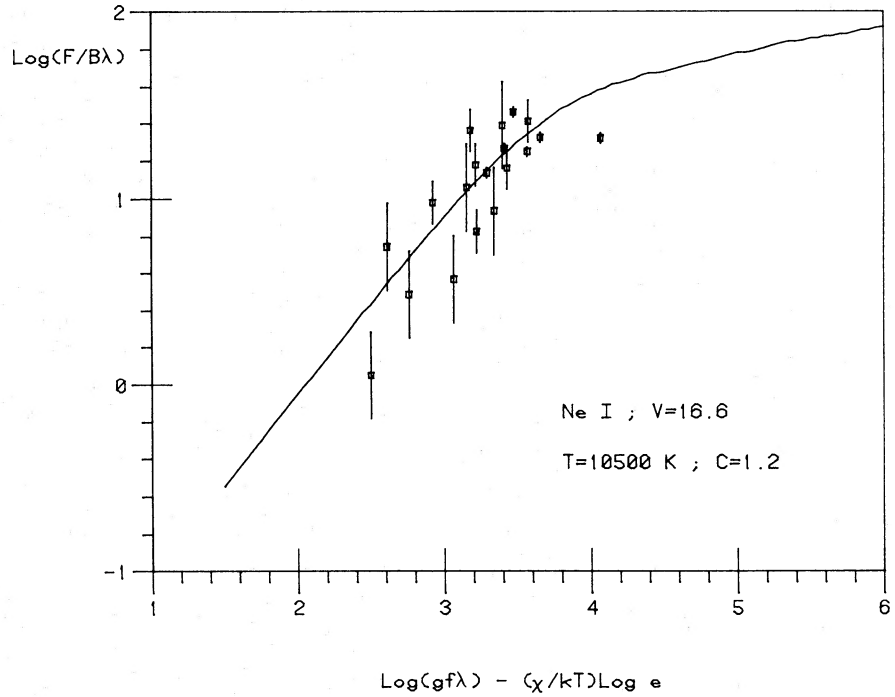

FIG. 5.—Same as Fig. 4, for Ne I emission lines. The horizontal shift of the theoretical curve is 8.45, and $\chi = 0$ for the reference energy level $2p^5 3s\ [1\frac{1}{2}]^o$ The data point on the extreme right is the line λ6402, which is weaker than expected.

we chose $F_0(\lambda 7143) = F(\lambda 7143)$ as a zero point.] By varying the reddening coefficient C and the effective temperature T over wide ranges, we minimized the scatter (χ^2) of the COG points around a third-order polynomial. The least scatter of the points for C II was found at $T = (1.05 \pm 0.1) \times 10^4$ K and $C = 1.2 \pm 0.1$.

Figures 4 and 5 show the COG for C II and Ne I, respectively, using the line flux data at the epoch $V = 16.6$. This is the only epoch at which the Ne I lines were prominent. (The solid curves in Figs. 4 and 5 are explained in § IV*f* below.) The Ne I energy levels and *gf*-values are from Wiese, Smith, and Glennon (1966). Each line is represented by a point, and the bar shows the uncertainty of the line flux. The COG for C II shows quite clearly the turnover point where the lines become optically thick, although this is based on only two points in this case $\lambda\lambda$6578, 6582, the strongest C II emission lines, as expected. This confirms the large optical depth expected for these lines from the strength of C II λ4740; see § IV*a* above. The slope of the best fitting straight line in the optically thin region of the curve is only $\sim 30°$, which is different from the expected value of 45°. Since the fluxes of the weak emission lines that comprise the left-hand part of the curve have large uncertainties, the deviation from the expected value of the slope is not a strong constraint on the conclusions, but rather indicates that the data may not be good enough to check fully the validity of the theory and idealized assumptions used here. The COG of the Ne I lines is rather insensitive to the temperature, since the emission lines in the visible region have lower levels very close in energy. In addition, since the Ne I lines cover only the spectral range 5800–7030 Å, the data points are not sensitive to the reddening correction either. Therefore we present the COG for Ne I using the same T and C values as obtained from the C II lines, assuming both sets of emission lines emerge from the same region.

We conclude that the C II and Ne I emission line region at the epoch $V = 16.6$ apparently is close to LTE at the above given temperature.

The scatter in similar COG plots for other epochs is large. It is possible that recombination, UV fluorescence, and dynamical gas flows are important when the star is bright, and therefore that the LTE approximation is no longer valid. On the other hand, at $V = 16.6$ the brightness was known to be rapidly declining (Heck, Houziaux, and Manfroid 1982). If the brightness decline was caused by the blocking of the central disk at $V = 16.6$ (see § V*a*), then the COG analysis for a chromosphere with no continuum background seems more nearly valid for that epoch than for others.

d) *The* Ne I *Emission*

To the best of our knowledge, the Ne I emission spectrum has never been observed previously in any astronomical object. The Ne I lines are also present in the CTIO spectra, where the [N II] lines were weak, so the Ne I emission is not correlated with the forbidden lines. On the other hand, while Ne I is very prominent at $V = 16.6$, the lines are very weak or absent near maximum, compared with C II and He I emission. The ionization potential of Ne^0 is 21.6 eV, which is close to, but below, the ionization potentials of C^+ and He^0. It therefore seems likely that the emissions of Ne I, C II, and He I all arise in the same region, namely the chromosphere of V348 Sgr. However, the difference in the ionization potentials may mean that Ne is relatively highly ionized in the bright phase, and hence that the Ne I lines are weak and below our noise level. The widths of the Ne I line profiles (see § III*b*) and their radial velocity indicates that their optical depth is smaller and they probably emerge from the whole chromospheric envelope, while the C II emission is more optically thick, and hence emerges primarily from nearer the edge of the (expanding) chromosphere. (This is also apparent from the COG analysis of § IV*c* above.) The only line of Ne I which clearly shows optical depth effects is λ6402, as seen in Figure 5.

e) *Reddening*

The H I Balmer decrement in the spectra of V348 Sgr can be used with some confidence to determine the reddening only at minimum light, when it appears that the H I photons are emitted mostly from the nebula. At other phases, there are uncertainties as to what fraction of the H I emission comes from each region of the object, and in addition, Hβ is blended with C II $\lambda\lambda$4862, 4867 (6). At $V = 18.4$, $H\alpha/H\beta = 5.8 \pm 1.0$ and $H\beta/H\gamma = 0.2 \pm 0.05$. Using the *AGN* values for case B at $T = 1.5 \times 10^4$ K and $N_e = 10^3$ cm^{-3} (see § IV*f* below), and the standard reddening curve, we obtain $E_{B-V} = 1.5$ from Hα/Hβ, and $E_{B-V} = 1.4$ from Hβ/Hγ.

The reddening value obtained from the C II COG best-fit procedure have $C = 1.2 \pm 0.1$, corresponding to $E_{B-V} = 0.9 \pm 0.1$. Houziaux (1968) found $E_{B-V} = 0.9$ from *UBV* observations. Reddening measurements in the galactic plane are reported by Neckel and Klare (1980). They found $E_{B-V} \approx 0.4$ in the vicinity of V348 Sgr. The presence of Na I interstellar absorption in its (CTIO) spectrum (§ III*f*) confirms that some portion of the reddening is interstellar. It is therefore possible that a large fraction of the reddening is intrinsic to the object, probably caused by a dust layer associated with the strong infrared emission (Webster and Glass 1974).

f) *The Forbidden-Line Region*

The strong [N II] + Hα emission lines in the spectrum of V348 Sgr near minimum probably arise in the envelope that gives it the nebulous appearance on the PSS red plate. Therefore we assume that the forbidden lines are emitted from a nebula surrounding a central object, and apply the theory of gaseous nebulae to that region (*AGN*). It is probable that the observed H I emission comes partly from this nebula and partly from the chromosphere.

The line intensity ratios [N II] (λ6583 + λ6548)/λ5754 and [S II] λ6717/λ6731 (corrected for the adopted reddening coefficient $C = 1.9$) give the temperature and density, respectively (although emission regions of [N II] and [S II] do not always coincide). From these lines, we find the values of $T \approx 2.1 \times 10^4$ K, $N_e \approx 10^3$ cm^{-3} for $V = 16.6$, and $T \approx 1.5 \times 10^4$ K and $N_e \approx 10^3$ cm^{-3} for $V = 18.4$. The density at $V = 16.6$ is uncertain since [S II] λ6716.4 is probably blended with Ne I λ6717.0. The temperature and density for brighter magnitudes could not be determined in this way, since λ5754 is weak and λ6730 is strongly blended with a C II quartet.

The doublet [O II] $\lambda\lambda$7320, 7330 is observed in emission at $V = 12.1$, when an infrared scan is available. While λ7320

is prominent, the strength of λ7330 is highly uncertain. It is probably present and certainly weaker than λ7320. Seaton and Osterbrock (1957) calculated the expected intensity ratio of the [O II] lines,

$$r'' = \frac{\lambda 3726 + \lambda 3729}{\lambda 7320 + \lambda 7330},$$

as a function of density and temperature. Our measured $\lambda 3726 + \lambda 3729 = \lambda 3727$ flux is quite uncertain, because of the atmospheric dispersion effects discussed above. Using $T = 2.1 \times 10^4$ K and $N_e = 10^3$ cm^{-3} (as obtained above), the calculated $r'' = 9.8$. The measured ratio, however, is roughly equal to 1. Even the higher reddening value obtained in § IV*e* above is not sufficient to account for that discrepancy. We conclude that this is another indication for the severe loss of ultraviolet photons on the slit jaws due to the atmospheric dispersion.

g) Abundances

i) *Abundances in the Chromosphere*

For that region we adopt the LTE approximation (see the Appendix and § III*c* above) and use the COG technique to get relative ion abundances for the epoch $V = 16.6$. First we plot the data using the results of the best fit for T and C as in Figures 4 and 5, and then fit the theoretical COG given by Powell (1969) by shifting one of his curves in the x and y directions. Since the data are not sufficient to distinguish between Powell's curves, we adopt the one with $a = 0.005$, since it has a prominent "flat" region. The horizontal shift found for C II is 5.2 ± 0.2, and the vertical shift is 6.4 ± 0.1. Since the dependence of ξ on the atomic mass is weak (see Appendix), we use the same *vertical* shift for the other ions. The horizontal shift for the Ne I COG is 8.45 ± 0.1.

From the LTE assumption the total number density N of an ion is given by

$$N = N_0 \frac{u}{g_0} \exp\left(\frac{-\chi_0}{kT}\right), \qquad (1)$$

where u is the partition function of the ion, and g_0 and χ_0 are the statistical weight and excitation energy (respectively) of the reference energy level. From (1) and from equation (9) of the Appendix, we get

$$\frac{N(C^+)}{N(Ne^0)} = \text{dex}\,[\Delta_h(Ne^0) - \Delta_h(C^+)] \times \frac{u(C^+)}{u(Ne^0)} \exp\left[\frac{\chi_0(C^+) - \chi_0(Ne^0)}{kT}\right].$$

Using the given horizontal shifts of the COGs of C^+ and Ne^0, the energies of their reference levels (Figs. 4 and 5), and $T = 1.05 \times 10^4$ K, we find $N(C^+)/N(Ne^0) = 4.3 \times 10^2$. Using similar methods for the few lines of He I and N II, assuming the same saturation level of the COG, we find $N(Ne^0)/N(C^+) = 0.85$, and $N(N^+)/N(C^+) = 2.4 \times 10^{-2}$. There are significant uncertainties in the COG procedure described above. The best-fit T and C values are accurate to within 10%. Along with the uncertainties in Powell's curve fitting (see above), we estimate that the results of the abundances ratios are accurate to within a factor of 2.

Examining the ionization potentials of the ions involved, we suggest that C and N are mostly in the form of C^+ and N^+. However, the degrees of ionization of Ne and He are highly uncertain, so their abundances ratio to C are probably higher than the above values by unknown amounts. The difference in the ionization potentials of Ne^0 and C^+ makes their relative ionization a function of the temperature, and of the ultraviolet radiation field in the chromosphere.

The abundance of H could not be determined in the COG method, since only three Balmer series lines are prominent, and their chromospheric flux is highly uncertain (see § IV*e*). At $V = 12.1$ (when the equivalent widths of the nebular emission lines were small), we find that the He I lines are comparable in flux to the H I lines; and since the excitation energy of the He I lines is much higher than that of H I, the number density of He^0 is probably higher than that of H^0. The degree of ionization of H is difficult to estimate, however, since the ultraviolet radiation field is unknown. Hence the abundance of H is unknown, but probably is in the order of the He abundance.

At $V = 16.6$, as well as at $V = 15$, the emission lines of S II and Si II are also prominent (Tables 2, 3). Since there are only a few prominent lines in the IDS spectra for these ions, a similar COG analysis could not be carried out. However, their number density must be nonnegligible.

ii) *Abundances in the Nebula*

The ratio of the forbidden-line fluxes to Hα are given by the equation (from *AGN*):

$$\frac{N(H^+)}{N(X^+)} = \frac{F(H\alpha)}{F(\text{line})} \frac{h\nu(\text{line})}{h\nu(H\alpha)} \frac{8.63 \times 10^{-6}\Omega(\text{line})}{T^{1/2} g_1} \frac{b}{\alpha_{H\alpha}^{\text{eff}}},$$

where Ω is the collision strength of the line, g_1 is the statistical weight of the ground level, $\alpha_{H\alpha}^{\text{eff}}$ is the effective recombination coefficient of Hα, and b is the fraction of the collisions that lead to the emission of a forbidden line photon. With $T = 1.5 \times 10^4$ K and $N_e = 10^3$ cm^{-3}, the line flux ratios [N II] λ6548/Hα and [S II] λ6730/Hα, measured at $V = 18.4$, give $N(N^+)/N(H^+) = (0.19 \pm 0.05) \times 10^{-5}$ and $N(S^+)/N(H^+) = (0.24 \pm 0.1) \times 10^{-5}$, respectively. Here we used the values for Ω, $\alpha_{H\alpha}^{\text{eff}}$, and b given at *AGN*, except for $b(\lambda 6730)$ which is calculated to be 0.19 (due to collisional de-excitations). No correction for reddening is needed here due to the proximity of the wavelengths.

The abundance of O is more uncertain because of the uncertainty in the flux of the doublet [O II] λ3727 (see § II). However, in order to get a crude estimate, we apply a reddening correction of $E_{B-V} = 1.0$ (§ IV*e*) and assume a constant slope of the continuum down to the ultraviolet, to obtain $F(\lambda 3727)/F(H\alpha) \approx 7.2$. We also assume that at the given density, $F(\lambda 3729)/F(\lambda 3726) = 0.8$. Using the critical densities given at *AGN* for these lines, we get $N(O^+)/N(H^+) = 0.24 \times 10^{-5}$. The probable error in the flux of λ3727 is 50%, hence the number density ratio is uncertain accordingly.

Since He I recombination lines are weak, the nebula is probably ionized by ultraviolet radiation with $h\nu < 24$ eV. Therefore O, S, and N are only singly ionized in the nebula, and their neutral-atom fractions are similar to the fraction of H^0, because of the similar ionization potentials. Therefore the abundances of these atoms relative to H are close to the number density ratios of the ions above. Those values

are all smaller than the solar abundances, but are intermediate compared with the range in abundances of various planetary nebulae (Torres-Peimbert and Peimbert 1977).

In summary, the nebula that has probably been expelled from the central object has somewhat lower metal abundance than the Sun. On the other hand, the chromosphere surrounding the central object is highly deficient in H, and consists primarily of C and He, with enhancement in N and Ne abundances.

V. IMPLICATIONS

a) General Structure

In this section we propose a tentative model of V348 Sgr, in an effort to account for its observed behavior and spectra.

The high abundance of C in the chromosphere clearly suggests a highly evolved star, which has already ejected its outer H-rich envelope and thus formed the observed nebula. According to the theory of the final stages of stellar evolution, C production and supply to the outer envelope are most efficient in the He shell flashing stage. When the envelope above the burning shell contains a relatively small fraction of the mass, it becomes quite extended and highly convective after the flash, and the processed materials are mixed outward (Paczyński 1977; Sackmann 1980; Iben *et al.* 1983). The C enrichment in C and He stars, although not as dramatic as in V348 Sgr, is similarly explained by a "dredge-up" mechanism based on convection (Paczyński 1975; Iben and Renzini 1982). The He shell flash occurs in stars with total mass less than 8 $M_\odot$. This is consistent with the radial velocity of V348 Sgr, which indicates an old Population I object with probably a relatively low mass.

The relatively high abundance of Ne can be explained in the same context. In the He-rich zone the original CNO nuclei have been converted predominantly to ^{14}N. The He burning process converts the ^{14}N primarily to ^{22}Ne via successive α-captures, so that in the layer beneath the He-burning shell the abundance of ^{22}Ne is of the order of the original CNO abundance (Iben 1975). Turbulent convection which reaches below the burning layer can bring the Ne outward into the envelope. Another possibility is very hot He-burning, which produces some ^{20}Ne by C/O burning in the flash. According to Iben (1975), the rate of *p*-capture on ^{12}C (hot CNO cycle) in the He-burning shell is proportional to the H abundance in the shell, and it can produce an overabundance of ^{14}N. The abundance of ^{14}N that Iben got in the convection shell of his model is on the order of the chromospheric N abundance of V348 Sgr (see § III*f*). However, the C and Ne abundances in his model are different, but they depend strongly on the detailed structure of the convection layer.

There is a long-standing question on the origin of the overabundance of ^{22}Ne in cosmic rays (Weidenbeck and Greiger 1981). Cassé and Paul (1982) try to explain it as resulting from Wolf-Rayet (hereafter W-R) WC stars which produce ^{22}Ne in their He-burning cores. V348 Sgr certainly provides direct evidence for the efficient production of Ne by He burning, although the isotope ratio (^{22}Ne/^{20}Ne) in the chromosphere of V348 Sgr is unknown and the star does not have the strong wind required to accelerate cosmic rays.

In light of the above, the observed chromosphere is probably a giant-like extended envelope that resulted from the expansion following a He shell flash. That might well be the very last flash, as suggested by Renzini (1981). Sackmann (1980) studied the evolution of a model of a 0.8 $M_\odot$ C/O core with an outer 0.015 $M_\odot$ C-rich envelope. After the flash, the outer envelope expanded dramatically in her model, especially because of the high opacity of C (see also Renzini 1981; Iben and Renzini 1982). In Sackmann's model, the temperature and density in the outer C-rich region dropped as low as 2.3×10^4 K and 1.6×10^{-13} g cm^{-3}, respectively. The conditions in the extended chromosphere observed in V348 Sgr are approximately similar. Iben *et al.* (1983) also explored the behavior of a pre–white dwarf undergoing a final He shell flash. The envelope in their model had higher effective temperature (in general) than V348 Sgr has, which probably resulted from the lower C abundance they adopted, and the resulting less extended envelope.

The time scale between the He shell flashes is on the order of 10^3 years (Paczyński 1975). That time scale is much too long to account for the observed brightness changes of V348 Sgr. The light curve actually resembles light curves of the R CrB group. Although the mechanism for their random luminosity drops is not fully understood (Feast 1975, 1979), we adopt the model of obscuration by dust clouds proposed for the R CrB group (O'Keefe 1939; Payne-Gaposchkin 1963), to account for the random light-curve variations of V348 Sgr. That model is favored in this particular case for the following reasons: (i) The high C abundance is a rich source for graphite dust particles. The time scale for dust formation can be as short as a few days (Krełowski 1975), and is proportional to the C abundance. (ii) The general structure of the emission spectrum of the chromosphere is similar at minimum and maximum light. It is hard to understand how the physical conditions would be preserved if the intrinsic luminosity varied dramatically. (iii) a correlation is observed between the continuum temperature and the luminosity (Table 1), in the sense that the thicker the obscuring dust is, the fainter and redder the object becomes. (iv) A strong infrared excess, with approximately constant luminosity, is observed in V348 Sgr (Webster and Glass 1974). This is strong support for a dust shell, which is probably nonuniform.

In general, it is not clear if the light curve variations of the R CrB stars are caused by orbiting clouds in the dust shell, or by newly formed compact clouds, which obscure part of the photospheric hemisphere, and subsequently expand to become optically thin (Feast 1975, 1979; Krełowski 1975). The dramatic drop in the continuum intensity at $V = 16.6$ and the large equivalent widths of the chromospheric emission lines at that time indicate a compact dust cloud obscuring most of the central hemisphere. As in a solar eclipse, the chromosphere remained partly visible, and the equivalent widths of the emission lines increased significantly. (Presumably the chromosphere of V348 Sgr is much more extended than the solar chromosphere.) The brightness came back up relatively shortly ($\sim$10 days) after the epoch of our observations at $V = 16.6$ (see light curve by Heck, Houziaux, and Manfroid 1982). This probably indicates that the cloud was compact and simply moved away from the line of sight, although visual brightening by rapid thinning of the (expanding) cloud cannot be ruled out.

There are two reasons to believe that the dust clouds are between the star and the surrounding nebula: (i) The emission intensity of the nebula is approximately constant during brightness changes. (ii) If we adopt a crude estimate for the minimum luminosity $M_V \approx -1$, based on the luminosity of the R CrB group and W-R central stars of planetary nebulae (see § V*b* below), the 8″ size of the resolved nebula corresponds to ~0.15 pc. Hence the quasi-period is too short to be explained by clouds located at that distance from the star. However, the large Balmer decrement in the nebula indicates the existence of additional dust within the nebula and around it.

The ionization mechanism of the nebula is not understood, since the ~B1 continuum (§ III*f*) has insufficient ultraviolet photons. We suggest the following alternatives: (i) The star was much hotter prior to the last He flash. The recombination time scale in the nebula is $\sim 10^3$ years, which is consistent with the (relatively short) interflash period. (ii) A small, hot companion exists which provides the necessary ultraviolet photons. Several planetary nebulae are known to have binary systems as their central stars (Livio 1982; Bond 1983). Although we have no evidence for a binary in V348 Sgr, we suggest high-speed photometric observations to check this point, as well as to look for possible short-period pulsations (like those found for RY Sgr by Alexander *et al.* 1972). (iii) The low ionization of the nebula (no He I or [O III] lines, therefore $h\nu \leq 24$ eV) coincides with the ionization stage of C, Ne, and He in the chromosphere. Those three ions can absorb most of the photons with $h\nu \leq 21$ eV and create a "cutoff" in the ultraviolet spectrum of the photosphere at that energy. Hence the existence of the planetary nebula arround V348 Sgr might indicate a hotter photosphere than suspected, with enough ultraviolet photons to achieve the low ionization in the nebula.

b) Comparison with Other Objects

Comparison of the properties of V348 Sgr with other related objects can contribute to further understanding of their nature.

i) The R CrB Stars

The light curves of stars of this group are very similar to V348 Sgr, although the latter has a shorter quasi-period, which probably indicates a smaller object. The R CrB stars are also believed to be old Population I stars, because of their kinematic properties. The inclusion of V348 Sgr in that group might indicate high luminosity and distance for it as well, which is consistent with its strong interstellar reddening. Strong infrared excesses are also observed in stars of the R CrB group (Feast and Glass 1973), and their spectra show H deficiency and high abundance of He and C (Herbig 1964; Schönberner 1975; Cottrell and Lambert 1982), although unlike V348 Sgr their atmosphere is dominated by He.

There are some major differences, however. The R CrB group are much cooler, red giant stars, with absorption spectra at maximum light, and they do not show planetary nebula–like emission. (However, Herbig 1964 suspected such emission in the spectrum of MV Sgr.) The spectra of R CrB itself at various phases are described in detail by Payne-Gaposchkin (1963). While the absorption spectrum is still present near minimum, strong chromospheric emission emerges, mainly Ca II H and K, Na I D, and strong λ3889, which is identified as He I. There is also evidence that these emission lines are still present at maximum light, although hidden by absorption. Payne-Gaposchkin also favored the dust-cloud obscuration model, suggested originally by O'Keefe (1939). But the difference from our picture of V348 Sgr is that in R CrB the clouds are supposed to be formed *beneath* the chromosphere, so that when the photosphere is blocked by the clouds, the chromosphere is prominent in emission.

The above differences can be explained as follows: The layer above the He-burning shell of V348 Sgr is less massive than in the R CrB stars. (It is not clear whether they already expelled their H-rich material as V348 Sgr did, since their cool atmospheres cannot ionize any presumed envelope.) As a result, the outer envelope of V348 Sgr is less extended, and its effective temperature is much higher. Consequently C is ionized in the outer region, and dust clouds cannot form in or below the chromosphere but only outside it. The overabundance of He in R CrB stars is probably responsible for the strong λ3889 emission lines, whose relative intensities with respect to other He I lines indicate small optical depths in the chrhomospheres. A smaller envelope mass can also explain the smaller size and higher C abundance of V348 Sgr. MV Sgr (Herbig 1964) might be an intermediate case between V348 Sgr and R CrB. Its suggested temperature is higher than R CrB, it shows C II (absorption), and its emission line spectrum below maximum light includes strong He I and (suspected) [N II].

Iben *et al.* (1983) try to associate their model of a white dwarf undergoing a thermal pulse with the R CrB phenomenon. The major difficulty with this idea is that the R CrB stars are much cooler than the effective temperature they calculated, and have no evidence of a planetary nebula–like envelope around them. V348 Sgr might be the missing link.

ii) The Old Population I W-R Group

Webster and Glass (1974) classified V348 Sgr as a possible "coolest" W-R star, based on its similarity in infrared emission with that group. The cool stars of the WC subgroup are believed to be embedded in dust shells (Allen, Swings, and Harvey 1972; Webster and Glass 1974). Some W-R stars are also known to be embedded in planetary nebulae (Aller 1956; Heap 1981). Smith and Aller (1971) presented very similar spectra of a W-R (WC8) star and the central star of a planetary nebula. Since the sequence of WC stars exhibits a continuous decrease in ionization and in Doppler broadening of the emission lines (see, e.g., Smith 1968; Heap 1981), V348 Sgr might well be a cooler extension of the WC subgroup, as suggested by Webster and Glass (1974). But this also implies a later evolutionary stage. Willis and Wilson (1978) suggest that WC stars are (younger) O stars burning He in their core. The C produced is carried out by mixing, at the same time the H-rich outer envelope is being stripped off by the observed strong wind. However, there are few observational differences between the young and massive W-R stars and the W-R central stars of planetary nebulae (see, e.g., Heap 1981). The latter group are believed to be fainter by ~4 mag, and their winds slower. Renzini (1981) suggested that the H-deficient WC central stars of planetary nebulae are actually very similar in structure to the He-shell burning model described in § V*a* above (but with hotter photospheres and higher He abundances).

So W-R central stars of planetary nebulae constitute a separate subgroup with probably different structures, masses, and evolutionary histories than the traditional massive W-R stars, which presumably burn He in their *cores*. Hence V348 Sgr could be thought of as a member of a cool extension of that subgroup, but actually its spectral characteristics (aside from the nebula) are somewhat closer to the R CrB group. Since Renzini (1981) and Iben *et al.* (1983) suggested a similar core evolutionary stage for both the W-R central stars and the R CrB group, V348 Sgr might be an important intermediate case between them.

VI. SUMMARY

V348 Sgr is unique in its joint characteristics of planetary nebulae, Wolf-Rayet stars, and R CrB stars. Its irregular behavior necessitates much further observation, especially high-resolution spectral and photometric monitoring over a relatively long period. We also strongly recommend high-speed photometry, to search for possible close-binary behavior. However, based on our observations and previous published results, we suggest that the object is the core of a giant star stripped of its outer layers. The stability of a white dwarf (or the central star of a planetary nebula) against a thermal pulse in the envelope depends on the core mass and the mass and composition of the outer envelope. We suggest that there is a sequence of increasing envelope mass from stable white dwarfs, through planetary nebulae with W-R WC central stars, V348 Sgr, and finally the R CrB group with their giant, extended envelopes. The uniqueness of V348 Sgr (and the rareness of the R CrB stars) implies that the mass margins are in fact quite small.

We would like to thank Dr. G. H. Herbig for suggesting this project to us, for many helpful discussions and ideas, and especially for allowing us to use his observations, reductions, measurements, and line identifications of the CTIO plates. We are most grateful to Dr. B. Paczyński for his careful reading of the manuscript and his enlightening suggestions. We are also grateful to Drs. H. E. Bond and J. M. Shuder for useful discussions. We would like to thank the National Science Foundation for partial support of this research under grant AST 79-19227, and for partially financing the Lick Observatory's VAX computer under grant AST 80-17504. One of us (D.E.O.) is grateful to the Guggenheim Foundation, for partial support under a Fellowship, and to the Institute for Advanced Study for its hospitality.

APPENDIX

The curve of growth (COG) theory for the intensities (not equivalent widths) of emission lines is based on the following assumptions: (*a*) The physical conditions of the emitting gas are close to LTE, and (*b*) a uniform temperature in the region is assumed.

From assumption (*a*) we apply Kirchhoff's law to get the intensity in an emission line,

$$E_\lambda = B_\lambda(T)[1 - \exp(-\tau_\lambda)], \tag{1}$$

where τ_λ is the optical depth at λ. For a turbulently widened line profile we have the total energy in the line

$$E(\text{line}) = B_\lambda(T)\Delta\lambda_D \int_{-\infty}^{+\infty} \{1 - \exp[-\alpha_0 NH(a, V)]\} dV ,$$

where the function $H(a, V)$ is the Hjerting function, $\Delta\lambda_D$ is the Doppler width of the line, N is the number density in the lower level, and

$$\alpha_0 = \frac{\pi^{1/2} e^2 f \lambda^2}{mc^2 \Delta\lambda_D} . \tag{3}$$

Thus we have

$$\frac{E(\text{line})}{B_\lambda(T)\Delta\lambda_D} = F(f, \Delta\lambda_D, N) . \tag{4}$$

So now

$$N = N_0 \frac{g}{g_0} e^{-\chi/kT} , \tag{5}$$

where N_0 is the number density in the reference energy level, g_0 is its statistical weight, and χ is the energy of the transition's lower level above the reference level. Therefore from (3) and (5) we get

$$\log(\alpha_0 N) = \log(gf\lambda) - \frac{\chi}{kT} \log e + C , \tag{6}$$

where

$$C = \log\left[\frac{N_0 \pi^{1/2} e^2}{g_0 \xi_0 mc}\right] . \tag{7}$$

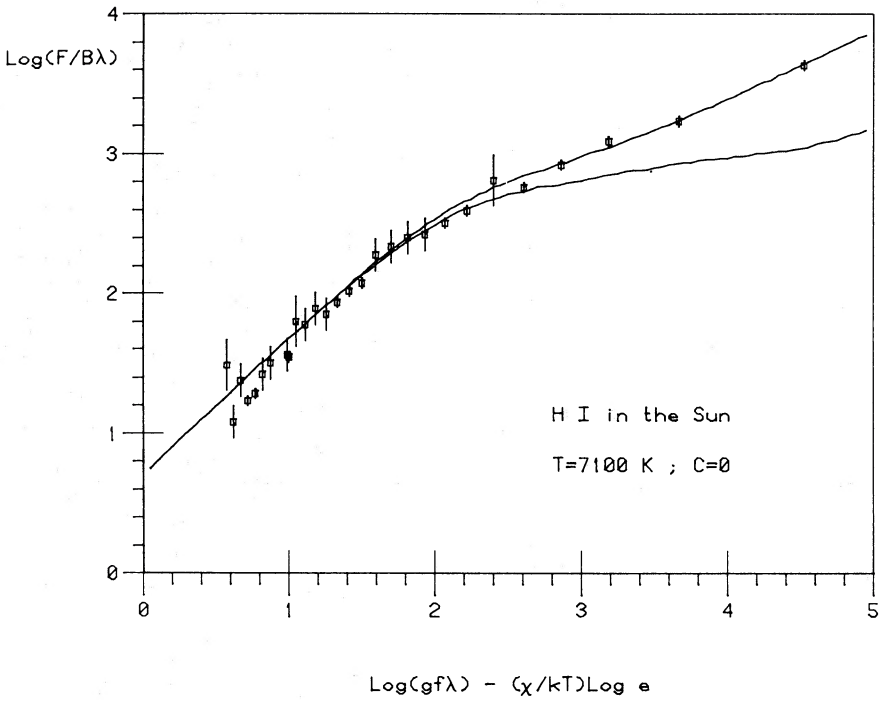

FIG. 6.—Curve of growth for H I emission lines in the solar chromosphere. $\chi = 0$ for the energy level $2p\,^2P^o$, and $T = 7.1 \times 10^3$ K. Upper solid curve is $a = 0.159$, and lower is $a = 0.005$ (see text). The curves are shifted by 6.8 horizontally and 7.5 vertically.

Here ξ_0 is the broadening velocity, and we also used

$$\Delta\lambda_D = \frac{\lambda\xi_0}{c} = \frac{\lambda}{c}\left[\frac{2kT}{Mc} + (\xi_T)^2\right]^{1/2}, \tag{8}$$

where ξ_T is the turbulent velocity, and M is the atomic mass.

We can now plot $\log [E(\text{line})/(B_\lambda(T)\lambda)]$ versus $\log (gf\lambda) - (\chi/kT) \log e$ to get the function F in (4), shifted in both axes when compared with Powell's (1969) standard curves. From equations (6) and (7), the horizontal shift is given by

$$\Delta_h = -\log\left(\frac{N_0}{g_0}\right) + C' \tag{9}$$

where C' is weakly dependent on the atomic mass M (eq. [8]).

The temperature T is a free parameter, and can be found by minimizing the χ^2 value of the scattered COG points around a third order polynomial.

In order to test the theory, we use the data from Dunn *et al.* (1967) for the H I Balmer series emission from the solar chromosphere. In Figure 6 we plot the COG for plate 76 of Dunn *et al.*, where we used the gf-values and energy levels from Wiese, Smith, and Glennon (1966), setting the reference energy level to be $2p\,^2P^o$. Obtaining the χ^2 best fit by the computer, we got $T = 7.1 \times 10^3$ K. The theoretical curve in Figure 6 was taken from Powell (1969), with $a = 0.159$, which best fitted the data. The curve $a = 0.005$ used for V348 Sgr emission lines is also plotted for comparison.

We are very grateful to Dr. G. Herbig for suggesting to us this treatment of the emission lines with the COG technique.

REFERENCES

Alexander, J. B., Andrews, P. J., Catchpole, R. M., Feast, M. W., Lloyd Evans, T., Menzies, J. W., Wisse, P. N. J., and Wisse, M. 1972, *M.N.R.A.S.*, **158**, 305.
Allen, C. W. 1963, *Astrophysical Quantities* (University of London).
Allen, D. A., Swings, J. P., and Harvey, P. M. 1972, *Astr. Ap.*, **20**, 333.
Aller, L. H. 1956, *Gaseous Nebulae* (London: Chapman & Hall), p. 205.
Bond, H. E. 1983, in *Cataclysmic Variables and Low-Mass X-ray Binaries*, ed. J. Patterson and D. Lamb (Dordrecht: Reidel), in press.
Cassé, M., and Paul, J. A. 1982, *Ap. J.*, **258**, 860.
Cottrell, P. L., and Lambert, D. L. 1982, *Ap. J.*, **261**, 595.
Dunn, R. B., Evans, J. W., Jefferies, J. T., Orrall, F. Q., White, O. R., and Zirker, J. B. 1967, *Ap. J. Suppl.*, **15**, 275.
Feast, M. W. 1975, in *IAU Symposium 67, Variable Stars and Stellar Evolution*, ed. V. E. Sherwood and L. Plaut (Dordrecht: Reidel), p. 129.
———. 1979, in *Changing Trends in Variable Star Research*, ed. F. M. Bateson, J. Smak, and I. H. Urch (Hamilton, N.Z.: University of Waibato), p. 246.
Feast, M. W., and Glass I. S. 1973, *M.N.R.A.S.*, **161**, 293.
Feldman, F. R., and MacAlpine, G. M. 1978, *Ap. J.*, **221**, 486.
Filippenko, A. 1982, *Pub. A.S.P.*, **94**, 715.
Glad, S. 1954, *Ark. Fys.*, **7**, 7.
———. 1956, *Ark. Fys.*, **10**, 291.
Grandi, S. A. 1975, *Ap. J.*, **196**, 465.
Heap, S. R. 1981, in *IAU Symposium 99, Wolf-Rayet Stars*, ed. C. de Loore and A. Willis (Dordrecht: Reidel), p. 423.

Heck, A., Houziaux, L., and Manfroid J. 1982, *Inf. Bul. Var. Stars*, No. 2184.
Herbig, G. H. 1958, *Ap. J.*, **127**, 312.
———. 1964, *Ap. J.*, **140**, 1317.
Hoffleit, D. 1958, *A.J.*, **63**, 78.
Houziaux, L. 1968, *Bull. Astr. Inst. Czechoslovakia*, **19**, 265.
Iben, I., Jr. 1975, *Ap. J.*, **196**, 525.
Iben, I., Jr., Kaler, J. B., Truran, J. W., and Renzini A. 1983, *Ap. J.*, **264**, 605.
Iben, I., Jr., and Renzini, A. 1982, *Ap. J.* (*Letters*), **259**, L79.
Johnson, H. 1965, *Ap. J.*, **141**, 923.
Kaler, J. B. 1976, *Ap. J. Suppl.*, **31**, 517.
Krełowski, J. 1975, in *IAU Symposium 67, Variable Stars and Stellar Evolution*, ed. V. E. Sherwood and L. Plaut (Dordrecht: Reidel), p. 149.
Livio, M. 1982, *Astr. Ap.*, **105**, 37.
Miller, J. S., Robinson, L. B., and Schmidt 1980, *Pub. A.S.P.*, **92**, 702.
Moore, C. E. 1970, *Selected Tables of Atomic Spectra* (*NBS* **3**, § 3).
———. 1975, *Selected Tables of Atomic Spectra* (*NBS* **3**, § 5).
Morgan, W. W., Keenan, P. C., and Kellman, E. 1943, *An Atlas of Stellar Spectra* (Chicago: University of Chicago Press).
Mühlethaler, H. 1977, Ph.D thesis, ETH Zurich.
Neckel, Th., and Klare G. 1980, *Astr. Ap. Suppl.*, **42**, 251.
Netzer, H., and Penston, M. V. 1976, *M.N.R.A.S.*, **174**, 319.
Nussbaumer, H., and Storey, P. J. 1981, *Astr. Ap.*, **96**, 91.
O'Keefe, J. A. 1939, *Ap. J.*, **90**, 294.
Osterbrock, D. E. 1974, *Astrophysics of Gaseous Nebulae* (San Francisco: Freeman) (*AGN*).
Osterbrock, D. E. 1981, *Ap. J.*, **246**, 696.
Paczyński, B. 1975, *Ap. J.*, **202**, 561.
———. 1977, *Ap. J.*, **214**, 812.
Payne-Gaposchkin, C. 1963, *Ap. J.*, **138**, 320.
Powell, P. L. T. 1969, *Roy. Obs. Bull.*, No. 152.
Renzini, A. 1981, in *IAU Symposium 99, Wolf-Rayet Stars*, ed. C. de Loore and A. Willis (Dordrecht: Reidel), p. 413.
Sackmann, I. J. 1980, *Ap. J.* (*Letters*), **241**, L37.
Seaton, M. J., and Osterbrock, D. E. 1957, *Ap. J.*, **125**, 66.
Seaton, M. J., and Storey, P. J. 1976, in *Atomic Processes and Applications*, ed. P. G. Burke and B. L. Moiseiwitsch (Amsterdam: North-Holland), p. 133.
Schönberner, D. 1975, *Astr. Ap.*, **44**, 383.
Smith, F. S. 1968, *M.N.R.A.S.*, **138**, 109.
Smith, L. F., and Aller, L. H. 1971, *Ap. J.*, **164**, 275.
Stone, R. 1974, *Ap. J.*, **193**, 135.
———. 1977, *Ap. J.*, **218**, 767.
Torres-Peimbert, S., and Peimbert, M. 1977, *Rev. Mex. Astr. Ap.*, **2**, 181.
Webster, B. L., and Glass, I. S. 1974, *M.N.R.A.S.*, **166**, 491.
Weidenbeck, M. E., and Greiger, D. E. 1981, *Ap. J.* (*Letters*), **247**, L119.
Wiese, W. L., Smith, M. W., and Glennon, B. M. 1966, *Atomic Transition Probabilities* (Washington: Government Printing Office) Vol. **1**.
———. 1969, *Atomic Transition Probabilities* (Washington: Government Printing Office) Vol. **2**.
Willis, A. J., and Wilson, R. 1978, *M.N.R.A.S.*, **182**, 559.

OVED DAHARI and DONALD E. OSTERBROCK: Lick Observatory, University of California, Santa Cruz, CA 95064